



저작자표시-비영리-변경금지 2.0 대한민국

이용자는 아래의 조건을 따르는 경우에 한하여 자유롭게

- 이 저작물을 복제, 배포, 전송, 전시, 공연 및 방송할 수 있습니다.

다음과 같은 조건을 따라야 합니다:



저작자표시. 귀하는 원저작자를 표시하여야 합니다.



비영리. 귀하는 이 저작물을 영리 목적으로 이용할 수 없습니다.



변경금지. 귀하는 이 저작물을 개작, 변형 또는 가공할 수 없습니다.

- 귀하는, 이 저작물의 재이용이나 배포의 경우, 이 저작물에 적용된 이용허락조건을 명확하게 나타내어야 합니다.
- 저작권자로부터 별도의 허가를 받으면 이러한 조건들은 적용되지 않습니다.

저작권법에 따른 이용자의 권리는 위의 내용에 의하여 영향을 받지 않습니다.

이것은 [이용허락규약\(Legal Code\)](#)을 이해하기 쉽게 요약한 것입니다.

[Disclaimer](#)

공학박사 학위논문

**Three-Dimensionally Interconnected
BCP/(PCL-Silica) Hybrid Scaffolds
with Controlled Microstructure for
Biomedical Implant**

제어된 미세구조와 3차원으로 연결된 기공 배열성을
갖는 생체의료용 인산칼슘/(폴리카프로락톤-실리카)

하이브리드 지지체

2012년 8월

서울대학교 대학원

재료공학부

최 원 영

Abstract

Three-Dimensionally Interconnected BCP/(PCL-Silica) Hybrid Scaffolds with Controlled Microstructure for Biomedical Implant

Won-Young Choi

Department of Materials Science and Engineering
Seoul National University

Porous bioceramics with aligned pores has been widely studied in bone tissue engineering field since they provide proper environment for bone cells to attach and grow, and three-dimensionally interconnected pore structures enable them to penetrate. Furthermore, porous bioceramic with adequate strength could be used as a supporting framework that can sustain loads as tissues grow. Among various methods of producing porous bioceramics, freeze casting has attracted great interest, as it can produce interconnected pore channels formed by freezing vehicles. The freezing vehicles can be easily removed by sublimation of frozen phase which in turn leaves pores in the ceramic body.

This present study reports novel, simple way of creating porous

BCP bioceramic scaffold with three-dimensionally interconnected pore structure by camphene-based freeze casting achieved by our recent works and suggests the potential application as biomedical implant by coating with organic/inorganic compound. First, porous BCP ceramic with unidirectional pore channels were produced by extruding frozen ceramic/camphene body through reduction die at room temperature. This simple extrusion process enabled the formation of aligned porous BCP ceramics as a replica of the camphene dendrites which were removed by freeze drying. The preferential orientation of pore structure was attributed to the extrusion process, which induced unidirectional elongation of camphene dendrite. Furthermore, for further application with diverse shapes of porous ceramic, fabrication of versatile designs of porous BCP ceramics were suggested by extruding frozen BCP/camphene body assembled with camphene rod as a shell and core, respectively. For the purpose of microstructure control, initial BCP contents and post-treatment time were changed, and the pore structure such as porosity, densification of BCP walls, pore size, and pore alignment were investigated.

However, the prepared porous BCP ceramics showed significantly enhanced mechanical strength in the parallel direction of pore alignment, but exhibited brittle fracture, due to the brittle nature of ceramic and porous structure. Therefore, our strategy is to coat the porous BCP ceramics with hybrid solution not only to enhance mechanical properties but also to provide biocompatible environment

for promising material that could be used in biomedical applications. The BCP/(PCL-silica) hybrid scaffolds could provide superior functions to conventional materials. In that point of view, we demonstrated fabrication of organic/inorganic hybrid composites. Poly(ϵ -caprolactone) was chosen as a biopolymer, which is most widely used polymer that can be degraded in human body and with biocompatibility. For inorganic compound in hybrid solution, sol-gel derived silica, which possesses the mesoporous structure, was used to improve bioactivity of the hybrid material. The PCL/sol-gel derived silica membrane with controlled pore structure were fabricated, characterized, and evaluated in assess of microstructure, wettability, and biological properties. The capability of antibiotic and protein loading was assessed for further applications in this work.

The potential of the BCP/(PCL-silica) hybrid scaffolds as the biomedical implant was examined by coating the porous BCP bioceramic scaffolds with prepared PCL/silica solution. Bone morphogenetic protein-2 (BMP-2) was loaded in the hybrid solution before coating the porous BCP bioceramic. The BCP(PCL-silica) hybrid scaffolds showed significantly improved fracture behavior, which could be used in load bearing part in biomedical field and the enhanced bioactivity of BCP(PCL-silica) hybrid scaffolds was examined by the in vitro cellular test using osteoblast-like cells. Furthermore, in vivo animal study was performed and osseointegration was examined using rat tibial defect model.

These results suggested that improved mechanical properties and enhanced biocompatibility could be achieved by PCL/silica solution coating on the porous BCP ceramic scaffold. Fabrication of antibiotic and grow-factor eluting material with controlled pore structure is another advantage of this work since in-situ loading of biomolecules to the coating solution is possible. The prepared BCP(PCL-silica) hybrid scaffolds by extrusion and coating process could be a promising material in biomedical applications.

Keywords: Porous, Freeze casting, Extrusion, Biomedical, Scaffold

Student Number: 2007-30811

Table of Contents

Abstract	i
Table of Contents	v
List of Tables	vi
List of Figures	vii
Introduction	1
1) Porous bioceramics as a bone scaffold	2
2) Production of porous bioceramics	5
3) The aim of this study	15
Fabrication of Porous BCP Ceramic Scaffold	19
1. Introduction.....	20
2. Experimental Procedure.....	22
3. Results and discussion	27
4. Conclusions.....	51
PCL-based Hybrid Scaffold	52
1. Introduction.....	53
2. Experimental Procedure.....	55
3. Results and discussion	59
4. Conclusions.....	75
GF/Drug-releasing Intelligent Hybrid Scaffold	76
1. Introduction.....	77
2. Experimental Procedure.....	82
3. Results and discussion	86
4. Conclusions.....	100
Conclusion	101
References	105

List of Tables

Table 1. Main characteristics of the solvents used for freeze casting and resulting characteristics of the pore structure

Table 1.1 Pore size and porosity of the cylindrical samples produced with various with BCP contents, before and after post-treatment

Table 1.2 Pore size and porosity of the tubular samples produced with various with BCP contents, before and after post-treatment

Table 1.3 Compressive strengths of the porous tubular BCP scaffolds with BCP contents of 15, 20, and 25vol%, before and after post-treatment.

Table 1.4 Compressive strengths of the multi-channeled porous BCP scaffolds with initial BCP contents of 15 vol%.

Table 3.1. Major classes of materials used as scaffold for bone growth factor [96]

Table 3.2. Types of growth factors [93]

List of Figures

Introduction

Figure 1. Schematic designs of various processing routes for the production of macroporous ceramics^[7]

Figure 2. Schematic diagram of freeze casting ^[12]

Figure 3. Processing steps of freeze casting^[19]

Figure 4. Macro and micro pores, freeze-cast alumina and HAp, respectively.^[19]

Figure 5. (A) Chemical structure and (B) DSC curves of camphene used in this study.

Figure 6. (A) Schematic diagram of extrusion process and (B) change of pore structure after extrusion of the frozen ceramic/camphene body.

Figure 7. Co-extrusion of frozen camphene and ceramic/camphene body through reduction die.

Figure 8. Features of calcium phosphate materials in wide range of fields^[27]

Part I. Fabrication of porous BCP ceramic scaffold

Figure 1.1. Schematic illustration showing the experimental procedure of the camphene based freeze-casting

Figure 1.2. Schematic diagram of multi-channeled porous BCP scaffold

Figure 1.3. Elongation of pores during extrusion process.

Figure 1.4. Representative SEM images of the porous cylindrical BCP scaffolds produced by extruding frozen BCP/camphene body after post-

treatment with various BCP contents of (A) 15vol%, (B) 20vol%, (C) 25vol%, and (D) before post-treatment.

Figure 1.5. Representative SEM images of the porous cylindrical BCP scaffolds after post-treatment at 33 °C, produced by extruding frozen BCP/camphene body with various BCP contents of (A)(B) 15vol%, (C)(D) 20vol%, (E)(F) 25vol%.

Figure 1.6. Representative SEM images at higher magnification of the porous cylindrical BCP scaffolds produced by extruding frozen BCP/camphene body with various BCP contents of (A)(D) 15vol%, (B)(E) 20vol%, (C)(F) 25vol%.

Figure 1.7. Schematic illustration showing the increase of pore size by post treatment of an extruded BCP/camphene body at 33 °C.

Figure 1.8. Representative SEM images of the porous tubular BCP produced by extruding frozen BCP/camphene body after post-treatment, with various BCP contents of (A) 15vol%, (B) 20vol%, (C) 25vol%, and (D) before post-treatment.

Figure 1.9. Representative SEM images of the porous tubular BCP scaffolds produced by extruding frozen BCP/camphene body after post-treatment, with various BCP contents of (A) 15vol%, (B) 20vol%, (C) 25vol%, and (D) before post-treatment in the direction of extrusion.

Figure 1.10. Representative SEM images of the (A) porous BCP scaffolds with multi-channels with BCP contents of 15vol%. Scaffolds with post-treatment for (B) 1, (C) 6, (D) 12, and (E) 24 hours.

Figure 1.11. Representative SEM images of the (A) porous BCP scaffolds with multi-channels with BCP contents of 15vol% in parallel direction of

extrusion. Scaffolds with post-treatment for (B) 1, (C) 6, (D) 12, and (E) 24 hours.

Figure 1.12. X-ray diffraction patterns of the samples (A) before sintering, and after sintering at (B) 1250 °C. (●: hydroxyapatite, ■: β -TCP, ▲: α TCP)

Figure 1.13. Pore size of the multi-channeled samples as a function of the post-treatment time at 33 °C. The digitally colored image of the sample produced with a post-treatment time of 24 h is shown.

Figure 1.14. Compressive strengths of the porous cylindrical BCP scaffolds with BCP contents of 15, 20, and 25vol%, before and after post-treatment.

Figure 1.15. Typical SEM images of the cells cultured for 1day on the porous BCP scaffolds with BCP contents of (A) 15, (B) 20, and (C) 25vol%.

Part II. PCL-based Hybrid Scaffold

: Hybrid Coating Materials for Efficient BMP Loading

Figure 2.1. Cross-sectional SEM images of the porous PCL/sol-gel derived silica membranes produced with various initial TEOS contents (A) 0, (B) 10, (C) 20, and (D) 30 vol%).

Figure 2.2. Porosity and pore size of the porous PCL/sol-gel derived silica membranes produced with various initial TEOS contents

Figure 2.3. EDS analysis of the porous PCL/silica hybrid membranes of (A) surface and (B) cross-section.

Figure 2.4. (A) TEM images and (B) EDS analysis of the porous PCL/silica hybrid membranes.

Figure 2.5. Chemical composition of the porous PCL/sol-gel derived silica

membranes produced with various initial TEOS contents(0, 10, 20, and 30vol%), by FT-IR

Figure 2.6. Water contact angle of the porous PCL/sol-gel derived silica membranes produced with various initial TEOS contents

Figure 2.7. Surface SEM images of the porous PCL/sol-gel derived silica membranes produced with various initial TEOS contents (A) 0, (B) 10, (C) 20, and (D) 30 vol%).

Figure 2.8. Cumulative drug release of the porous PCL/sol-gel derived silica membranes produced with various initial TEOS contents

Figure 2.9. CLSM Visualization of the growth factor by green fluorescence with various initial TEOS contents, (A) 10, (B) 20, and (C) 30vol%

Figure 2.10. (A) Viability of the cells on the membrane after culturing for up to 5 days, (B) alkaline phosphatase activity(ALP) of the MC3T3 cells.

Part III. GF/Drug-releasing Intelligent Hybrid Scaffold

Figure 3.1. Representative SEM images of the porous BCP scaffolds coated with hybrid solution with BCP contents of (A)(D) 15, (B)(E) 20, and (C)(F) 25 vol%, showing infiltration of the hybrid solution.

Figure 3.2. Representative SEM images of the porous BCP scaffolds coated with hybrid solution with BCP contents of 15vol%, showing coating of the hybrid solution.

Figure 3.3. Compressive strength of the porous BCP scaffold with various BCP content, before and after hybrid solution coating.

Figure 3.4. Confocal laser scanning microscopy images of GFP adsorbed porous hybrid BCP scaffold.

Figure 3.5. Cumulative amounts of BMP released from the PCL/(PCL-silica) hybrid scaffold as a function of time.

Figure 3.6. CLSM images of the porous hybrid BCP scaffold produced using various conditions, (A) bare BCP scaffold, (B) PCL/silica coated, and (C) PCL/silica/BMP loaded.

Figure 3.7. Cell viability and ALP activity of the PCL/(PCL-silica) hybrid scaffold with various conditions.

Figure 3.8. Photograph of surgical procedure.

Figure 3.9. Representative 2D radiographs of control, PCL/silica coated, and PCL/silica/BMP-2 coated scaffold in tibia at 0 and 4 weeks of surgery.

Introduction

1) Porous bioceramics as a bone scaffold

In bone tissue engineering, bone implants serve as substrates for migration, proliferation, and differentiation of cells infiltrated from the surrounding tissues followed by the tissue ingrowths into the pores. In particular, since the combination of cells within the extracellular matrix characterizes any vital tissue in the body, one of the main in vivo functions of the biomedical implant is to act as a scaffold for cell adhesion, proliferation and additional extracellular matrix deposition which allow tissues to grow. Therefore, an adequate scaffold is crucial for biomedical application. The ideal scaffold should be three-dimensional; porous with an interconnected pore network; biocompatible and non-toxic to allow cell adhesion, proliferation and differentiation; biodegradable with a controlled degradation rate; and should have proper mechanical properties.

In this manner, the three-dimensional (3D) porous scaffold made of bioceramics plays an important role in biomedical field due to the following advantages: 1) they provide biocompatible surface and a large interfacial area to bone cell to grow^[1], 2) enable bone cell penetration and promote rapid bone growth throughout the interconnected pores ^[2], and 3) possess proper mechanical properties to sustain loads as bone tissues grow^[3]. For this issue, a number of works on three-dimensional biocompatible porous bioceramics with an interconnected pore network has been reported^[456]. The properties of porous bioceramics can be tailored by controlling the composition and microstructure of the porous bioceramics. Changes in open and closed

porosity, pore size distribution, and pore morphology can have a major effect on the properties of scaffolds. These microstructural features are manipulated by the various processing methods used to produce the porous bioceramics. The replica of polymer foams by impregnation methods, sacrificial template, and direct forming are of particular interest in fabrication methods, as shown in Fig 1.[⁷] Since the biological and mechanical properties of porous materials are strongly affected by their pore structure, the precise control and capability of tailoring the pore formation is one of the most crucial aspects in this field[⁸]. Therefore in this study, three-dimensional porous bioceramic scaffolds with interconnected pore network are produced by camphene-based freeze casting and the microstructural features are investigated.

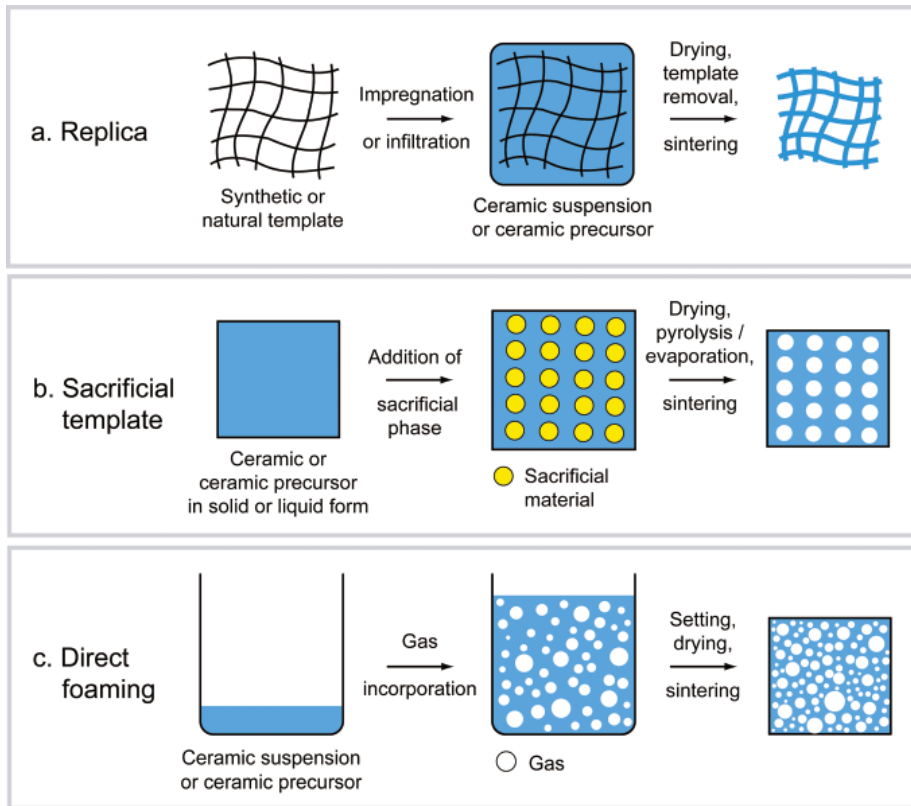


Figure 1. Schematic designs of various processing routes for the production of macroporous ceramics[7]

2) Production of porous bioceramics

Considerable efforts have been given to the development of fabrication methods to produce porous ceramics with controlled pore structure. One of the most promising techniques to produce porous ceramics is freeze casting^[9, 10, 11]. Freeze-casting is a wet-shaping technique, of which the preparation of well-dispersed and stable colloidal suspension is involved^[12], as illustrated in Fig. 2. and has received a great deal of attention during past few years. Basically, this technique is consisted of preparing a colloidal suspension, freezing a liquid suspension in a mold, sublimation of the solidified phase, and subsequent sintering to densify the walls, as summarized in Fig 3. Four types of ingredients are required for the preparation process of a colloidal suspension, ceramic powder, solvent, functional additives, and processing additives. The pores are formed as a replica of frozen solvent, in other words freezing vehicle, such as water^[13], camphene^[14, 15, 16], and TBA^[17, 18]. The characteristics of various freezing vehicles are summarized in Table 1. The pore structure is primarily defined by the choice of the solvent, the solidification conditions, morphology of the growing dendrites of freezing vehicle and packing of the ceramic particles between the dendrites. The most striking feature of the freeze-casting is the directionality of the pores, which is formed under proper freezing conditions. The solidification of freezing vehicle is performed directionally, resulting in materials with macro and micro pores running along the solidification direction.(Fig. 4^[19]) Furthermore, high compressive strength can be achieved by preferential growth of ice dendrite during freezing, for example, using double-side cooling

[²⁰], polymeric additives [²¹], and electric field [²²].

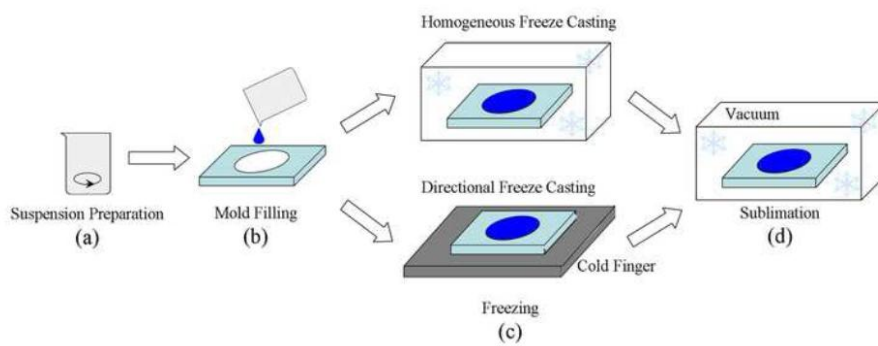


Figure 2. Schematic diagram of freeze casting [12]

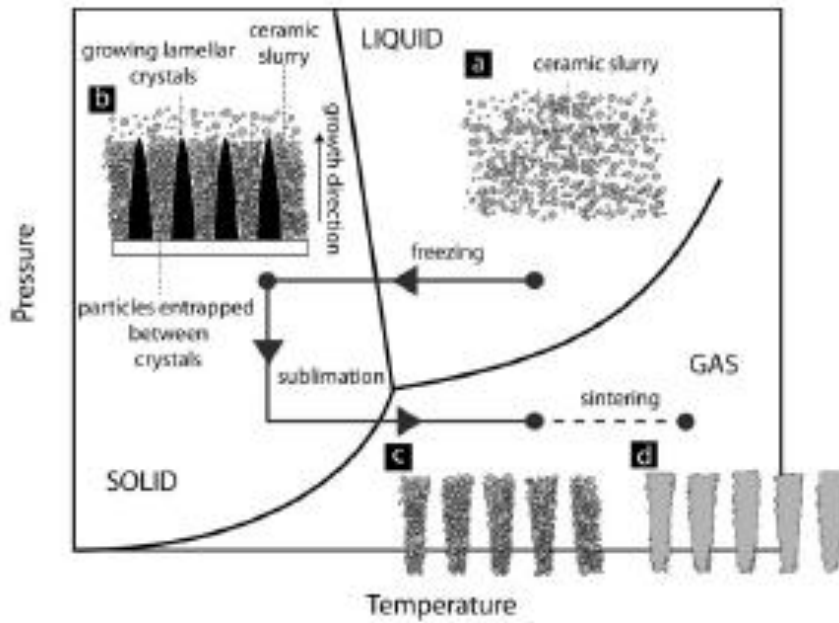


Figure 3. Processing steps of freeze casting[19]

Solvent	Water	Camphene	Tert-butyl alcohol
Solidification temperature	0°C or lower	30 - 50°C	25.3°C
Slurry preparation temperature	Room temperature	60°C	Room temperature
Pores morphology	Lamellar channels	Dendritic channels	Prismatic channels

Table 1. Main characteristics of the solvents used for freeze casting and resulting characteristics of the pore structure

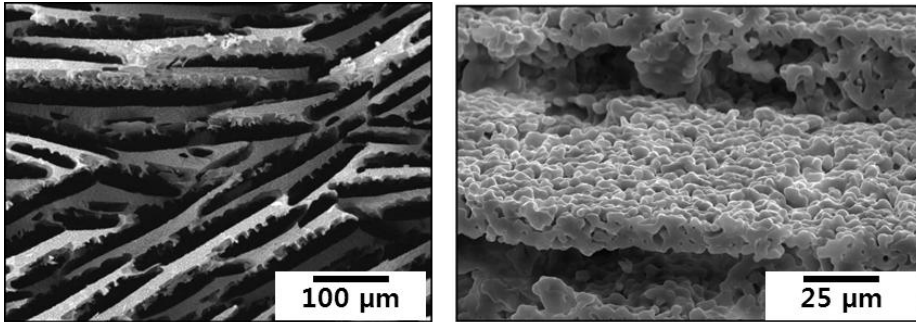


Figure 4. Macro and micro pores, freeze-cast alumina and Hap, respectively[19].

In the case of camphene as a freezing vehicle, freezing of ceramic/camphene slurry and postal process can be carried out at near room temperature, due to the moderate solidification temperature of camphene. In detail, camphene($C_{10}H_{16}$ 2,2-dimethyl-3-methylenebicyclo [2,2,1] heptane)(Fig 5(A)) is a crystalline plastic solid at room temperature which is one of the most striking features of the camphene, thus allowing the extrusion of frozen ceramic/camphene body even at room temperature (usual $T_s=30-50^{\circ}C$, $35-39^{\circ}C$ for camphene used in this study)(Fig 5(B)). Extrusion is a simple process used to create objects of a fixed cross-sectional profile. A material is pushed or drawn through a die of the desired cross-section. During the extrusion process, the camphene dendrite would extensively elongate, enabling the formation of highly aligned pores(Fig 6). In addition, co-extrusion process can be also applied in camphene-based freeze-casting simply by inserting core rod while freezing the ceramic/camphene slurry(Fig 7). Co-extrusion is the extrusion of multiple layers of material simultaneously. This type of extrusion utilizes two or more extruders to deliver a steady volumetric throughput of different viscous plastics to a single extrusion die which will extrude the materials in the desired form.

However, due to the high porosity and preferentially oriented pore network, mechanical strength of the porous bioceramics in normal direction of the pore alignments was usually low^[23]. The limitation of the scaffold strengths narrows the ranges of applications, so it is one of the major challenges in fabrication of porous bioceramic scaffold. Therefore, a number of researches were focused on the improving the mechanical strength

of porous bioceramic scaffold [6, 24]. In this study, coating with biopolymer/inorganic mixture is proposed to complement the limited application of porous ceramic scaffold due to low mechanical strength.

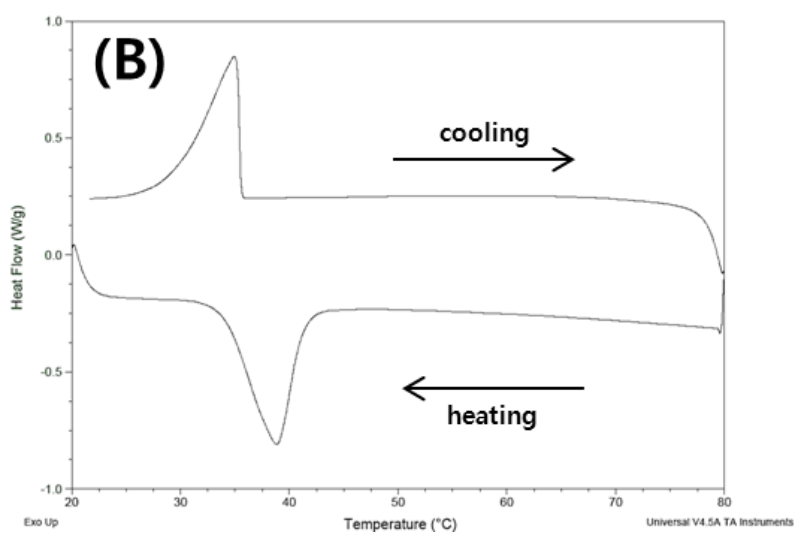
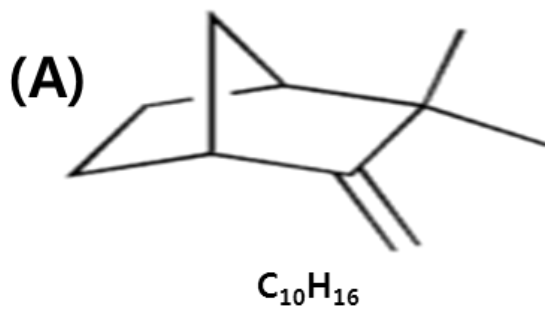


Figure 5. (A) Chemical structure and (B) DSC curves of camphene used in this study.

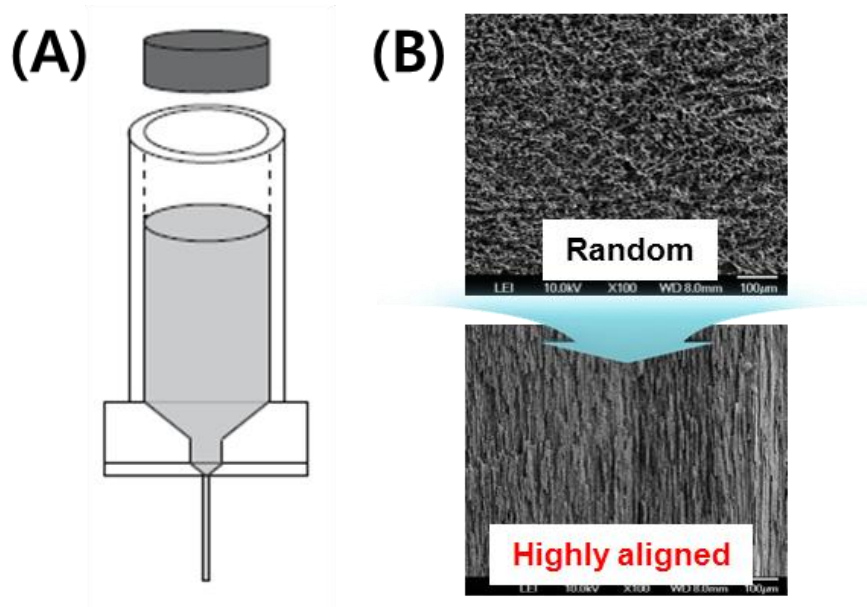


Figure 6. (A) Schematic diagram of extrusion process and (B) change of pore structure after extrusion of the frozen ceramic/camphene body.

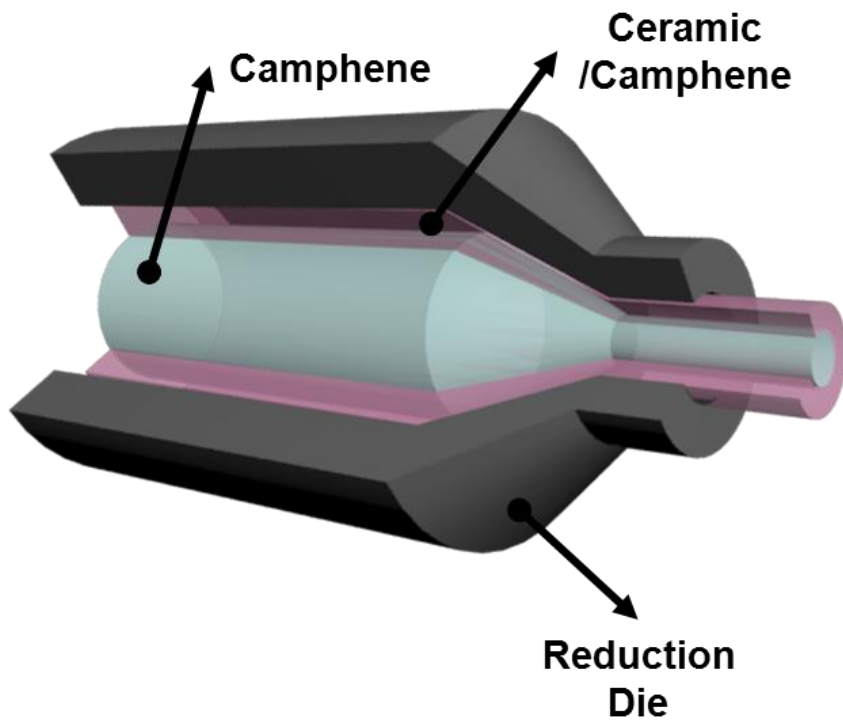


Figure 7. Co-extrusion of frozen camphene and ceramic/camphene body through reduction die.

3) The aim of this study

This present study reports novel, simple way of producing three-dimensionally interconnected BCP/(PCL-silica) hybrid scaffolds with controlled microstructure for biomedical implant. The production of highly aligned porous BCP ceramic scaffold with interconnected pore network was achieved by extruding frozen BCP/camphene body, followed by the coating process of organic/inorganic hybrid solution to improve the scaffold strength and provide biocompatible surface with functionality. First, porous BCP bioceramic scaffold with three-dimensionally interconnected pore structure was produced by camphene-based freeze casting achieved by our recent works. Porous BCP ceramic with unidirectional pore channels were produced by extruding frozen ceramic/camphene body through reduction die at room temperature, which would extensively elongate the camphene dendrites. Post-treatment at 33 °C, which is close to the solidification temperature of camphene, allowed camphene dendrites in the extruded body to overgrow continuously, was performed. Biphasic calcium phosphate (BCP) was used as bioceramic since BCP is one of the most widely used bioceramic due to its excellent bioactivity, biocompatibility and osteoconduction [25](Fig 8), which is consisted of a mixture of hydroxyapatite (HA) and b-tricalcium phosphate (b-TCP). The osteoconduction and subsequent new born formation would be stimulated when the scaffolds are porous and have three-dimensionally interconnected pores [2]. Therefore, the porous BCP bioceramic scaffold was produced by camphene-based freeze casting. The pore structure was tailored by controlling initial BCP content in BCP/camphene slurry, using

binder to prevent cracks that are generally caused by shrinkage. In addition, since the porous bioceramic scaffold requires proper strength to be used as a supporting framework^[26], extrusion of frozen BCP/camphene was imposed to elongate camphene dendrite in preferential orientation, consequently aligned pore structure, and heat treatment of frozen ceramic/camphene body at a temperature close to solidification temperature of camphene to gain dense BCP walls. For their potential use as scaffold, the examinations were performed via pore characteristics, such as pore size, porosity, and mechanical properties to evaluate their structural integrity. The biocompatibility of scaffolds was evaluated by preliminary osteoblastic activity using MC3T3 cells. It should be noted that scaffold with a three-dimensional interconnected pore structure with high porosity, large surface area, and biocompatibility is integral for application in tissue engineering.

In addition, the potential of PCL-silica hybrid solution as the coating material for biomedical application is examined as a membrane type. Biomolecules, such as tetracycline hydrochloride and bone morphogenetic protein-2 (BMP-2) was loaded in the hybrid solution in situ. Poly(ϵ -caprolactone) was chosen as a biopolymer, which is most widely used polymer that can be degraded in human body and with biocompatibility. For inorganic compound in hybrid solution, sol-gel derived silica, which possesses the mesoporous structure, was used to improve bioactivity of the hybrid material. The PCL/sol-gel derived silica membrane with controlled pore structure were fabricated, characterized, and evaluated in assess of microstructure, wettability, and biological properties. The capability of

antibiotic and protein loading was assessed for further applications in this work.

The potential of the BCP/(PCL-silica) hybrid scaffolds as the biomedical implant was examined by coating the porous BCP bioceramic scaffolds with prepared PCL/silica solution. Bone morphogenetic protein-2 (BMP-2) was loaded in the hybrid solution before coating the porous BCP bioceramic. The BCP(PCL-silica) hybrid scaffolds showed significantly improved fracture behavior, which could be used in load bearing part in biomedical field and the enhanced bioactivity of BCP(PCL-silica) hybrid scaffolds was examined by the in vitro cellular test using osteoblast-like cells. Furthermore, in vivo animal study was performed and osseointegration was examined using rat tibial defect model. Fabrication of antibiotic and growth factor eluting material with controlled pore structure is another advantage of this work since in-situ loading of biomolecules to the coating solution is possible. The prepared BCP(PCL-silica) hybrid scaffolds by extrusion and coating process could be a promising material in biomedical applications.

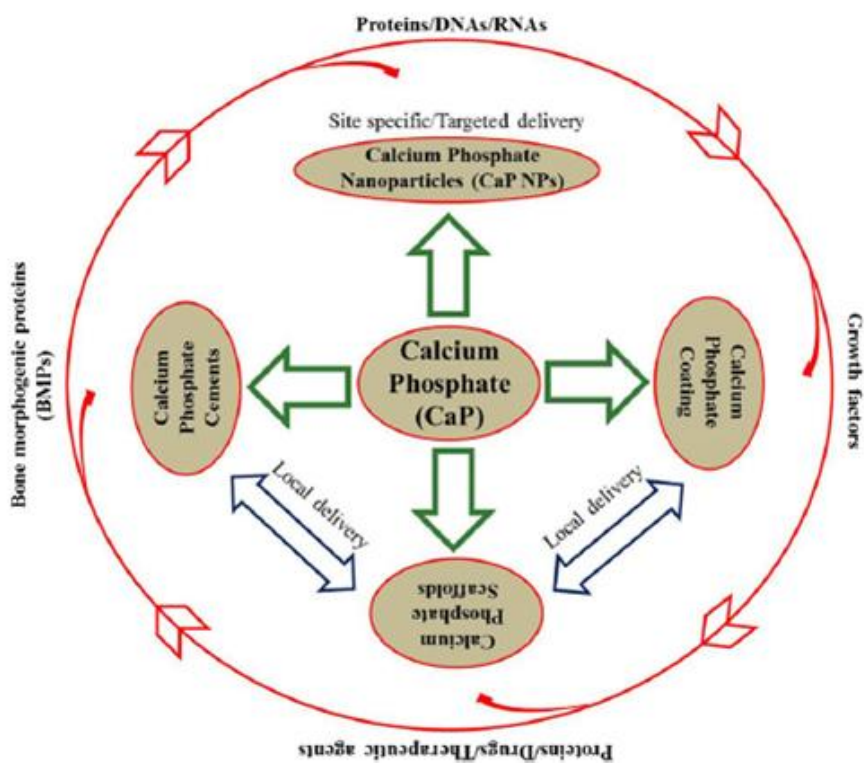


Figure 8 Features of calcium phosphate materials in wide range of fields. [27]

Part I.

Fabrication of Porous BCP Ceramic Scaffold

1. Introduction

Porous bioceramics with aligned pores has been widely studied in bone tissue engineering field since they provide proper environment for bone cells to attach and grow, and three-dimensionally interconnected pore structures enable them to penetrate^[28,29,30]. Furthermore, porous bioceramic with adequate strength could be used as a supporting framework that can sustain loads as tissues grow^[31]. These great advantages can be achieved by tailoring some of parameters in producing procedures, because these properties are strongly dependent on their pore structure^[32]. Various methods to impart porous structure to a ceramic are reported such as replica method^(33,34), gel-casting^[35,36], and freeze casting^[3,37]. These methods have attracted great interest due to their potential of controlling the pore structure, therefore considerable efforts has been made to enhance the capability of controlling the pore structure and improve the properties of porous bioceramics^[24, 38].

Among these methods, freeze casting has been emerged as a strong candidate, as it can produce interconnected pore channels formed by freezing vehicles. These freezing vehicles can be easily removed by sublimation of frozen phase which in turn leaves pores in the ceramic body. Usually ceramic/camphene slurry is prepared by ball-milling and cast into the mold at a temperature close to vehicle's solidification point. Great efforts have been made to control and adjust the porous structure of ceramic body by manipulating the dendrite growth during freezing.

Our group has focused on the capability of constructing pores by

using ceramic/camphene slurry, where frozen camphene dendrite could be deformed into arbitrary designs at room temperature. The pore structure could be tailored by controlling initial ceramic content in ceramic/camphene slurry, using binder to prevent cracks that are generally caused by shrinkage, post-treatment of frozen ceramic/camphene body at a temperature close to solidification temperature of camphene, and extruding to elongate camphene dendrite in preferential orientation. In this study, we propose a novel, simple way of producing porous ceramics with aligned pores by extruding frozen BCP/camphene slurry with various designs for customized applications via cylindrical, tubular, and multi-channeled porous BCP ceramics. For their potential use as scaffold, the examinations were performed via pore characteristics, such as porosity, interconnection size, and mechanical tests to evaluate their structural integrity. It should be noted that scaffold with a three-dimensional interconnected pore structure with high porosity, large surface area, and biocompatibility is integral for application in tissue engineering.

2. Experimental Procedure

Fabrication of porous BCP ceramic scaffold

Commercially available biphasic calcium phosphate (BCP, OssGen Co., Gyeonbuk, Korea) which was comprised of ~ 60wt% hydroxyapatite (HA) and 40wt% tricalcium phosphate (TCP) phases and camphene (C₁₀H₁₆, Alfa Aesar/Avocado Organics, Ward Hill, MA, USA) were used as the ceramic and freezing vehicle in this study, respectively. All of the reagents were used as received without any treatment or further purification.

The experimental procedures for camphene-based freeze-casting are briefly illustrated in Fig 1.1. Highly aligned porous BCP scaffolds with a range of BCP contents (15, 20, and 25 vol%) were produced freeze casting and extrusion. To accomplish this, the BCP powder was warm ball-milled with molten camphene and 3 wt% of an oligomeric polyester dispersant (Hypermer KD-4, UniQema, Everburg, Belgium) at 60 °C for 24 hours, to be used as a shell. The BCP/camphene slurry was cast into a pre-cooled mold with dimensions of 20 mm in diameter for cylindrical type. All of the samples were frozen at 3 °C for solidification of camphene. The frozen BCP/camphene body was extruded through a reduction die with an orifice of 3 mm diameter. This allowed the preferential orientation of camphene dendrite along the direction of extrusion. Subsequently, the extruded green bodies were heat-treated at 33 °C for 3 hours in oven, and then placed in freeze dryer remove the solid camphene by sublimation for 24 hours. Freeze dried samples were then sintered at 1250 °C for 3 hours to densify the BCP walls. For tubular type, BCP/camphene slurry was cast into a pre-cooled mold with prepared

cylindrical camphene rod of ϕ 10mm placed in the center. For multi-channelled design, 10mm x 10mm camphene rod was placed in the center, and then extruded through reduction orifice of 5mm x 5mm with an initial BCP content of 15vol%. 16 of 1st passage extruded bodies were assembled and re-extruded with same reduction die to produce 2nd pass extruded body(Fig 1.2).

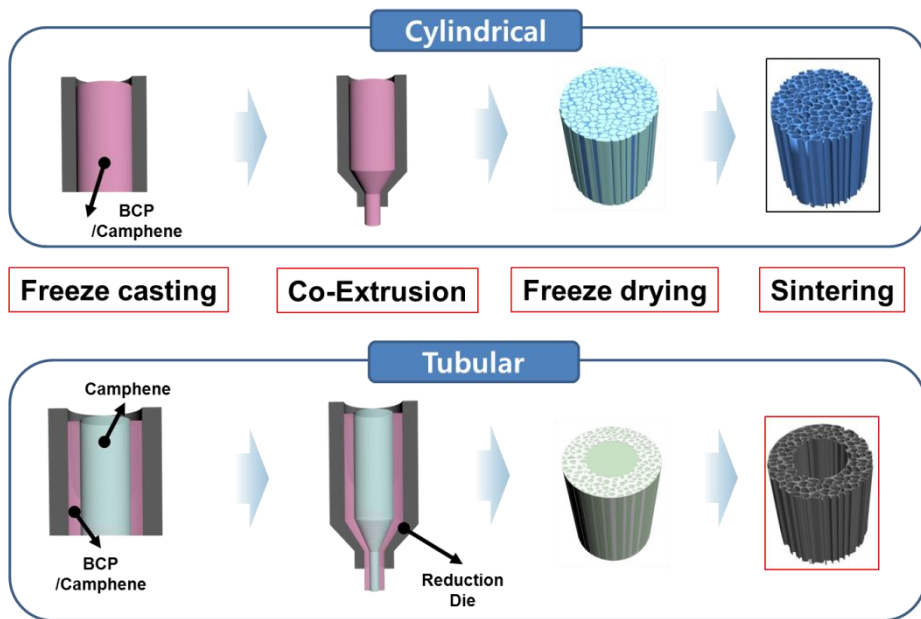


Fig 1.1 Schematic illustration showing the experimental procedure of the camphene based freeze-casting

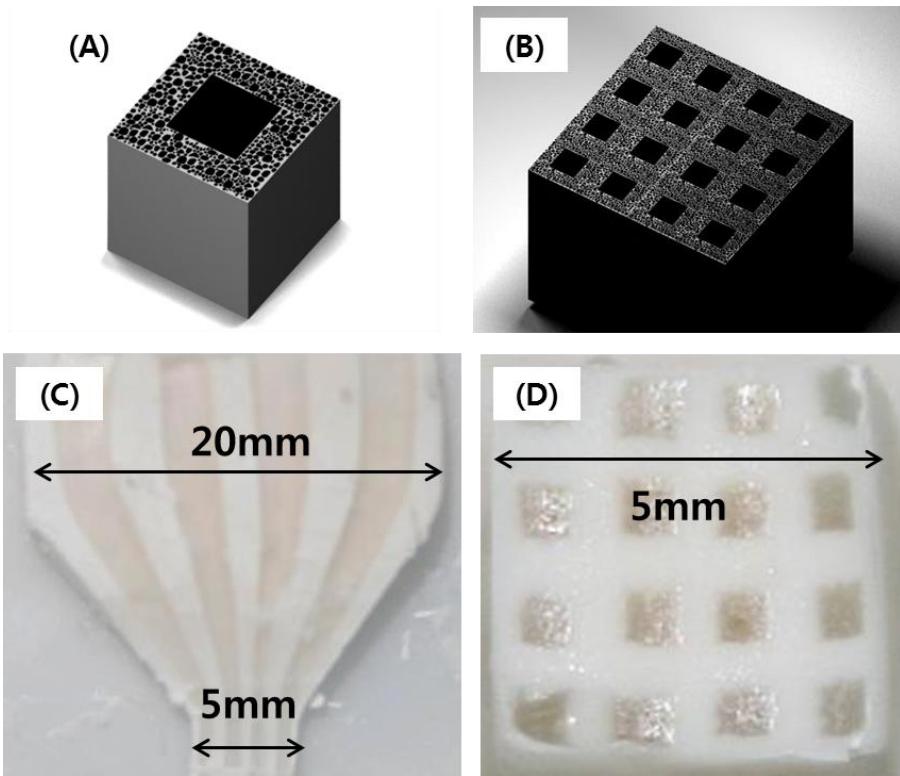


Figure 1.2. Schematic diagram of multi-channeled porous BCP scaffold

Characterization

The pore structures of the fabricated samples were characterized by field emission scanning electron microscope (FE-SEM, JSM6701F, JEOL Technique, Japan). Porosity, pore size, degree of pore alignment, pore interconnection, and microstructure of BCP walls were observed. The pore size and interconnections between the pores of the scaffolds was calculated roughly from the SEM images of the samples and porosity from its dimensions and weight. The crystallinity of the as-received and sintered sample was characterized using X-ray diffraction (XRD, MXP18A-HF, MAC Science, Japan)

Mechanical properties

For the purpose of mechanical tests, compression strength test and 3-point bending test were performed in accordance of screw driven load frame (OTU-05D, Oriental TM Corp., Korea). The samples with dimensions of ϕ 2.9 mm x ~ 6 mm were compressed parallel to the direction of pore alignment, loaded at a pressing speed of 1 mm/min and load-extension data were obtained from six samples and used to calculate an average value and its standard deviation of compressive strength.

Cellular response

Preliminary osteoblastic activity of the cylindrical samples was evaluated by in vitro cell test. The MC3T3-E1 cell line (ATCC, CRL-2593) was used to characterize the initial attachment behavior of the cells. Prior to

seeding cells, the samples were sterilized with 70% ethanol for 30 minutes and then dried on a clean bench under ultraviolet (UV) irradiation for 12 hours. The preincubated cells were plated at a density of 5×10^4 cells/ml and cultured in a humidified incubator in an atmosphere containing 5% CO₂ at 37°C. Minimum essential medium (α -MEM: Welgene Co., Ltd., Seoul, Korea) supplemented with 10% FBS, 1% penicillin-streptomycin was used as the culturing medium. The cell attachment was observed by SEM after culturing for 1day.

3. Results and discussion

Porous BCP ceramics with highly aligned pores were produced successfully by extruding frozen BCP/camphene body. In particular, the camphene dendrite grew and elongated unidirectionally during extrusion process(Fig 1.3), which transformed into pores after sublimation by freeze drying, with preferential orientation parallel to the direction of extrusion. In addition, it was possible to control pore structure and degree of alignment by adjusting the initial BCP content in the BCP/camphene slurry. The mechanical properties of samples were also affected due to the densification of pore walls.

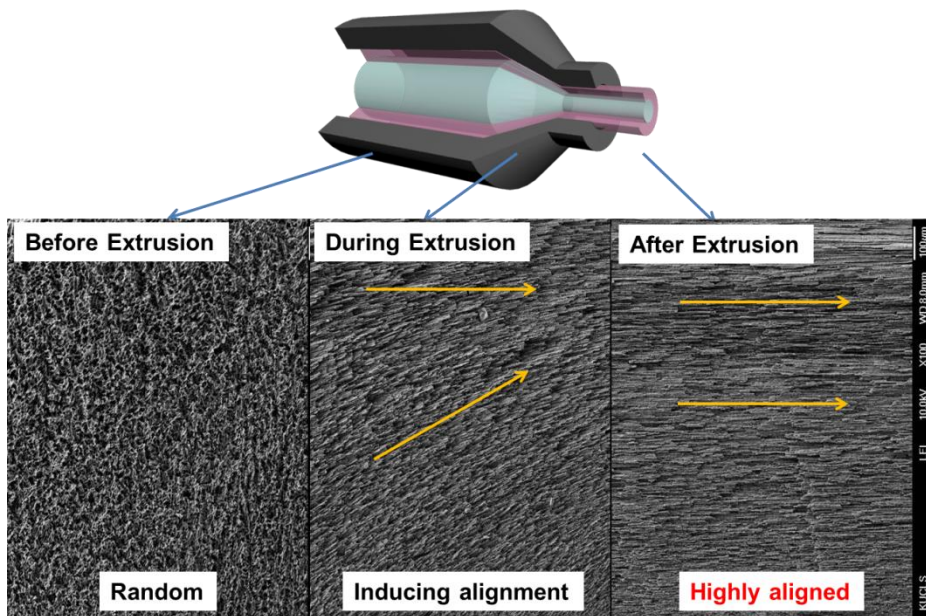


Figure 1.3. Elongation of pores during extrusion process.

Microstructure observation & Characterization

Fig 1.4, 1.5, and 1.6 shows the microstructure of the cylindrical samples produced with various content of an initial BCP content of 15, 20, and 25vol% before and after post-treatment, in parallel and normal direction of extrusion, respectively. All of the samples showed highly aligned pore structure. Fabricated samples without heat treatment showed relatively large pores and porous BCP walls even after sintering at 1250°C for 3 h. Well aligned pores were formed as a replica of the camphene dendrite by extrusion which elongated and deform frozen BCP/camphene body unidirectionally. On the other hand, samples with heat treatment at 33°C, pores became larger while preserving the pore alignment, as shown in Fig 1.7. After post treatment of extruded body, pores became significantly larger, which is attributed by heat treatment close to the solidification temperature of BCP/camphene slurry, at which camphene dendrite continuously grew during heat treatment^[15] and the BCP ceramics were more closely packed, which resulted in aligned pores and dense pore walls(Fig 1.6). In addition, the porous structure of the porous BCP ceramics was strongly affected by the initial BCP content in the range of 15 to 25 vol%. Regardless of the initial BCP content, all of the fabricated samples showed an aligned porous structure formed as a replica of unidirectionally grown camphene dendrites^[39]. The samples with an initial BCP content of 15 vol% showed relatively large sizes of pores and interconnections. As BCP contents increased, pore sizes decreased due to the smaller portion of camphene dendrite which formed pores after removal. However, as expected, the pore size of the sample

decreased with increase of an initial BCP content. Similar trend was observed for tubular scaffolds as shown in Fig 1.8 and 1.9.

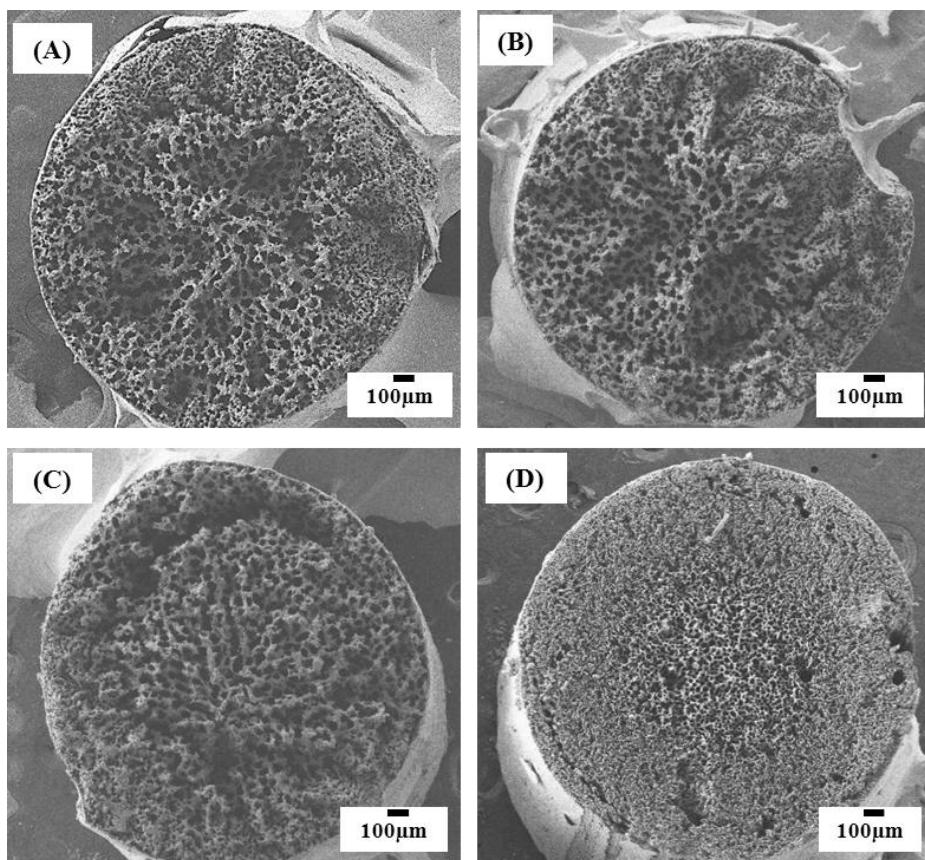


Figure 1.4. Representative SEM images of the porous cylindrical BCP scaffolds produced by extruding frozen BCP/camphene body after post-treatment with various BCP contents of (A) 15vol%, (B) 20vol%, (C) 25vol%, and (D) before post-treatment.

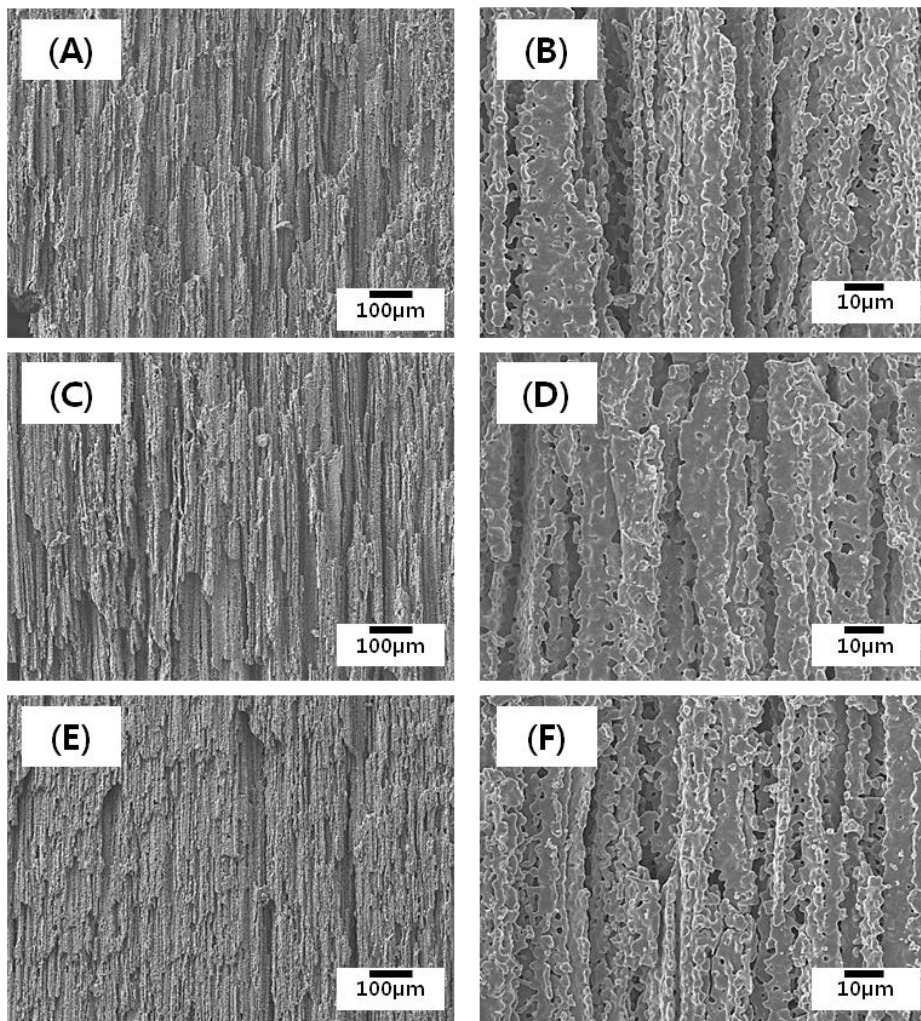


Figure 1.5. Representative SEM images of the porous cylindrical BCP scaffolds after post-treatment at 33 °C, produced by extruding frozen BCP/camphene body with various BCP contents of (A)(B) 15vol%, (C)(D) 20vol%, (E)(F) 25vol%.

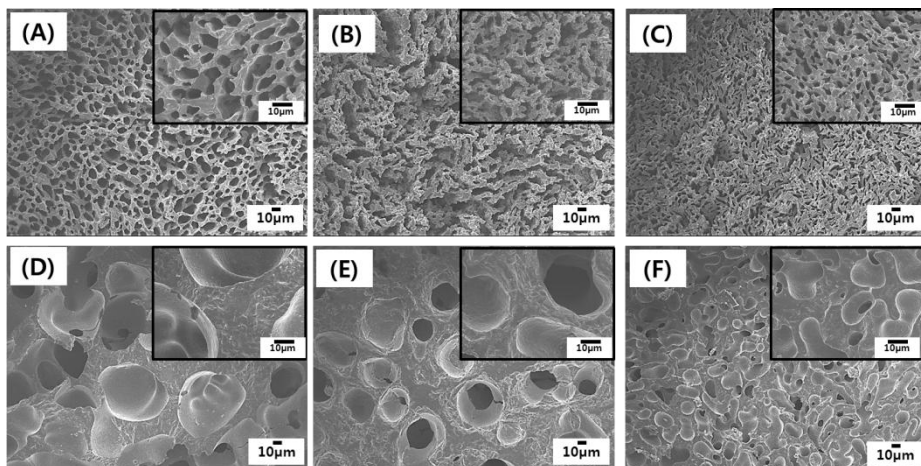


Figure 1.6. Representative SEM images at higher magnification of the porous cylindrical BCP scaffolds produced by extruding frozen BCP/camphene body with various BCP contents of (A)(D) 15vol%, (B)(E) 20vol%, (C)(F) 25vol%.

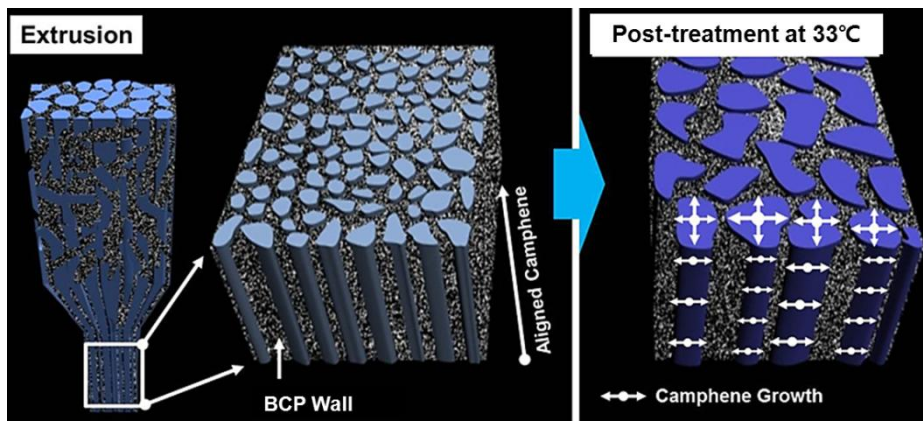


Figure 1.7. Schematic illustration showing the increase of pore size by post treatment of an extruded BCP/camphene body at 33°C.

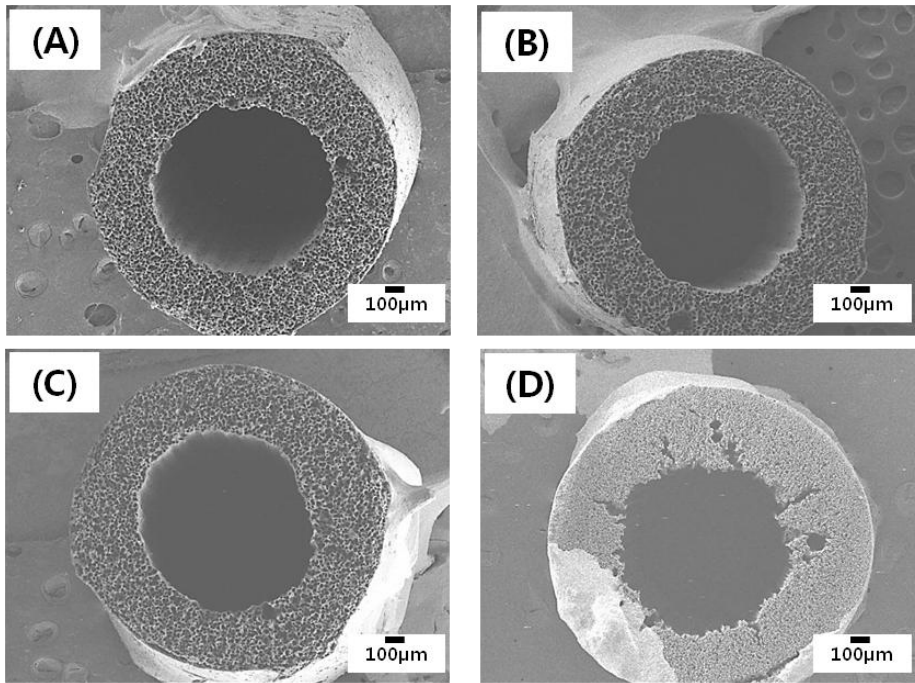


Figure 1.8. Representative SEM images of the porous tubular BCP produced by extruding frozen BCP/camphene body after post-treatment, with various BCP contents of (A) 15vol%, (B) 20vol%, (C) 25vol%, and (D) before post-treatment.

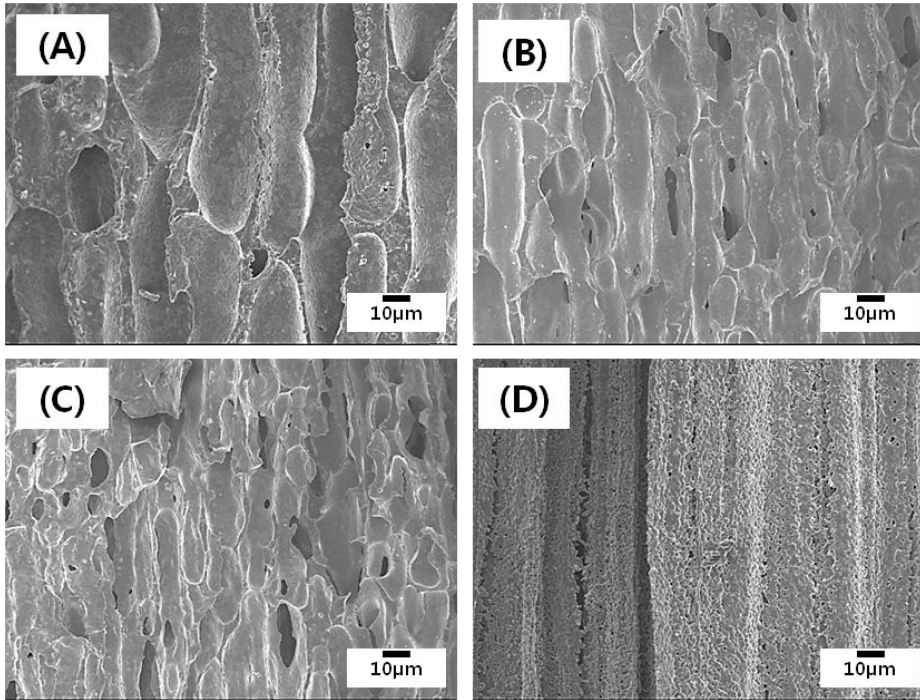


Figure 1.9. Representative SEM images of the porous tubular BCP scaffolds produced by extruding frozen BCP/camphene body after post-treatment, with various BCP contents of (A) 15vol%, (B) 20vol%, (C) 25vol%, and (D) before post-treatment in the direction of extrusion.

In vitro, lower porosity stimulates osteogenesis by suppressing cell proliferation and forcing cell aggregation. In contrast, *in vivo*, higher porosity and pore size result in greater bone ingrowth^[37]. In recent *in vitro* and *in vivo* studies, various pore sizes and proper pore interconnections are recommended for sufficient vascularization^[40]. In this manner, for further application as biomedical implant, complex design of porous BCP scaffold is proposed as multi-channel design which possesses macro pore channels and micro pores. Representative SEM images of the multi-channeled porous BCP scaffolds with heat treatment at 33°C, produced by extruding frozen BCP/camphene body with BCP contents of 15vol% is shown in Fig 1.10 and 1.11. The aligned porous structure was preserved even after 2nd passage of 16 assemblies of 1st extruded body. However, multi-channeled porous BCP scaffold showed a number of defects such as void and crack, which were formed during 2nd passage of extrusion, as shown in Fig 1.10.(A). It should be noted that there was no specific treatment after assembling 16 assemblies. These defects could be overcome by heat treatment before 2nd passage extrusion, wherein the partial remelting of the frozen bodies could occur, which would allow the good bonding of camphene dendrites at the interfaces. The porous structure of the porous BCP ceramics was strongly affected by the post-treatment time, while preserving the aligned porous structure, as shown in Figs 1.11.

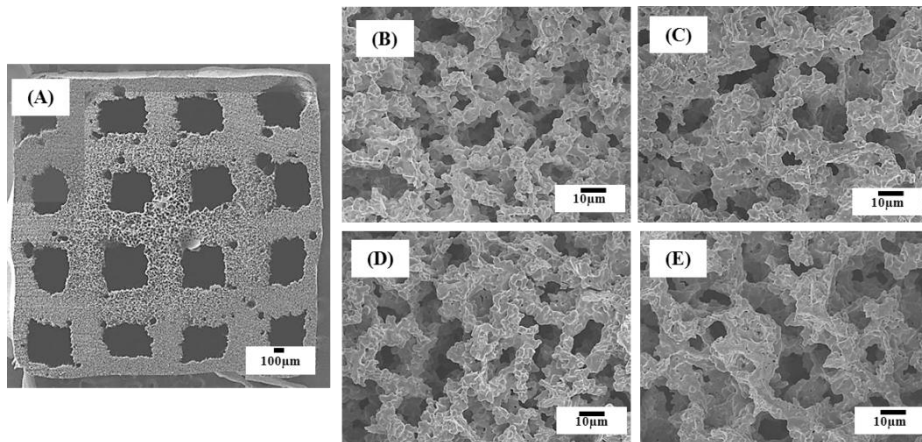


Figure 1.10. Representative SEM images of the (A) porous BCP scaffolds with multi-channels with BCP contents of 15vol%. Scaffolds with post-treatment for (B) 1, (C) 6, (D) 12, and (E) 24 hours.

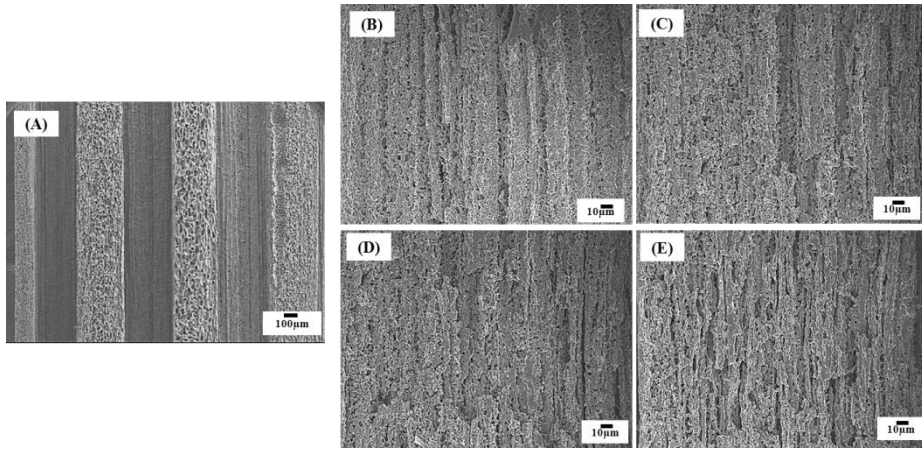


Figure 1.11. Representative SEM images of the (A) porous BCP scaffolds with multi-channels with BCP contents of 15vol% in parallel direction of extrusion. Scaffolds with post-treatment for (B) 1, (C) 6, (D) 12, and (E) 24 hours.

The crystallization behaviors of the samples before and after sintering were characterized using XRD analyses, as shown in Fig 1.12. As expected, the green sample showed the typical XRD pattern of hydroxyapatite and β -TCP phase without any noticeable crystal peaks. After sintering at temperature of 1250 °C, sample showed crystallization peaks corresponding to hydroxyapatite, β -TCP, and 3% of α -TCP phase. Formed α -TCP(α -tricalcium phosphate, α -Ca₃(PO₄)₂) phase is a metastable phase which is prepared from β -TCP at sintering temperature above 1125 °C^[41]. The Seo, DS and co-workers reported the formation of α -TCP phase at grain boundaries of HA^[42]. The relative content α -TCP was calculated from XRD analysis using the following index;

$$\text{Index} = \frac{I_{\alpha\text{-TCP}(170)}}{I_{\text{HA}(211)} + I_{\beta\text{-TCP}(0210)} + I_{\alpha\text{-TCP}(170)}}$$

where $I_{\beta\text{-TCP}(0210)}$ is the peak corresponding to (0210) intensity of β -TCP, $I_{\text{HA}(211)}$ is the peak intensity of HA, and $I_{\alpha\text{-TCP}}$ the peak intensity of (170) of (170) crystal plane of α -TCP.

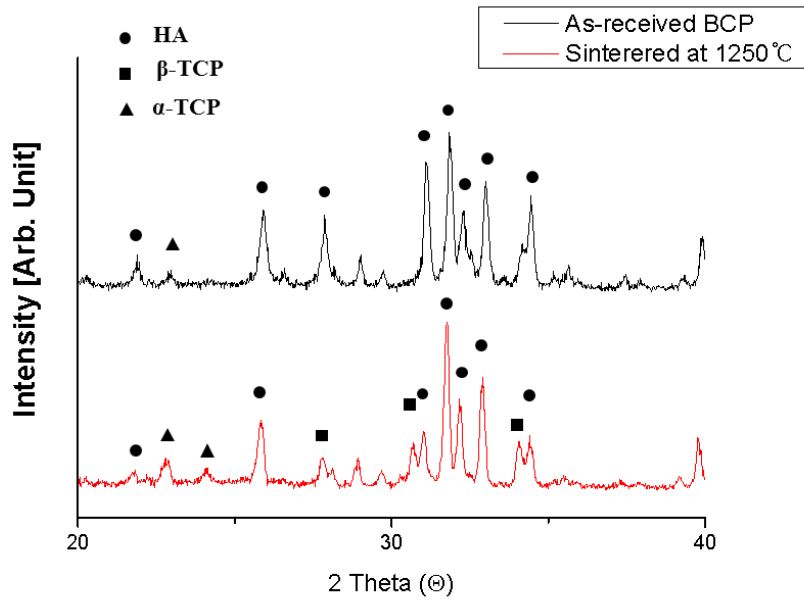


Fig 1.12. X-ray diffraction patterns of the samples (A) before sintering, and after sintering at (B) 1250 °C. (●: hydroxyapatite, ■: β -TCP, ▲: α TCP)

Pore Characterization

The porosity and pore structure are known as major factors affecting the properties of porous scaffold, in the bone tissue engineering applications [43]. The pore structure characteristics of the porous cylindrical BCP ceramics with various initial BCP contents were calculated from the SEM images and summarized in Table 1.1. The pore size and porosity increased notably after heat treatment at 33 °C, which would be beneficial for cellular activities. Meanwhile, the pore size decreased remarkably from $73.6 \pm 11.5 \mu\text{m}$ to $31.9 \pm 5.4 \mu\text{m}$ with an initial BCP contents increasing from 15 to 25 vol%. Decreased pore size would play an important role in cellular development, type of cells attracted, and the orientation and directionality of cellular ingrowth [4]. In addition, these decreases in the pore size attributed by larger portion of BCP framework would be expected to improve the mechanical properties. However, the porosity showed negligible difference, which suggest continuously grown camphene dendrite were preserved even after heat treatment.

Table 1.1 Pore size and porosity of the cylindrical samples produced with various with BCP contents, before and after post-treatment

BCP (vol%)	Before Post-Treatment		After Post-Treatment	
	Pore size [μm]	Porosity [vol%]	Pore size [μm]	Porosity [vol%]
15	23.6 ± 7.4	70.8 ± 4.6	73.8 ± 11.5	70.2 ± 4.6
20	9.2 ± 3.6	62.5 ± 3.8	49.4 ± 10.7	62.2 ± 3.4
25	5.9 ± 3.3	54.7 ± 6.6	31.9 ± 5.4	55.3 ± 0.7

The pore size and porosity of the porous BCP tubular ceramics with various initial BCP contents were also calculated from the SEM images and summarized in Table 1.2. The core part of the tubular BCP was omitted in the calculation of porosity. The pore size increased and porosity showed negligible difference after heat treatment. Meanwhile, the pore size was smaller than that of cylindrical scaffold, which is attributed to the assembly of camphene rod in the center. No noticeable defects, such as cracking and distortion were observed between the interface of BCP/camphene body and camphene rod. These results suggest that porous BCP scaffold with aligned structure could be fabricated in arbitrary designs and the pore characteristics could be controlled by various conditions in the producing process. For example, a similar trend was observed for multi-channeled samples (Fig. 1.13). Heat treatment allowed the densification of pore walls by the continuous growth of camphene dendrite, and the extrusion process provided elongated camphene dendrite in a preferential direction, which would be, in turn, expected to improve the mechanical properties. However, the porosity showed negligible difference, which suggests that continuously grown camphene dendrites were preserved even after heat treatment.

Table 1.2 Pore size and porosity of the tubular samples produced with various with BCP contents, before and after post-treatment

BCP (vol%)	Before Post-Treatment		After Post-Treatment	
	Pore size [μm]	Porosity [vol%]	Pore size [μm]	Porosity [vol%]
15	20.6 ± 4.4	72.0 ± 1.1	36.8 ± 9.2	71.8 ± 4.1
20	19.2 ± 4.6	64.6 ± 3.7	31.4 ± 7.7	65.3 ± 1.0
25	17.9 ± 2.3	60.9 ± 2.6	24.2 ± 3.4	61.1 ± 6.1

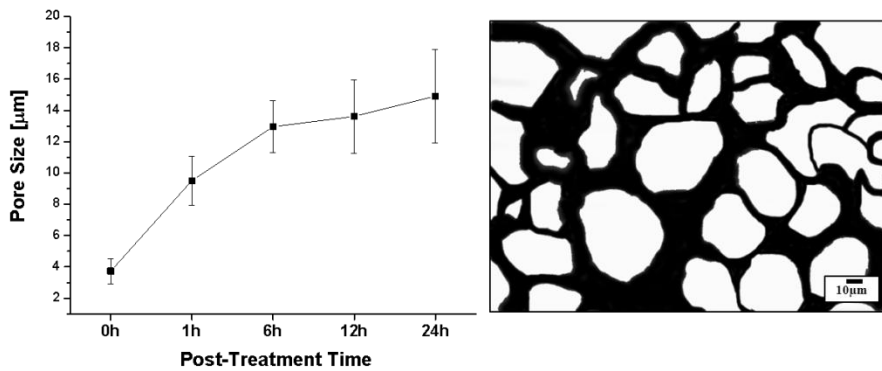


Fig 1.13 Pore size of the multi-channelled samples as a function of the post-treatment time at 33 °C. The digitally colored image of the sample produced with a post-treatment time of 24 h is shown.

Mechanical Properties

In order to examine the effect of the degree of pore alignment and initial BCP content on the mechanical properties of the aligned porous BCP scaffolds, compressive strength tests were carried out. Loads were applied in parallel and normal direction of pore alignment in compressive strength test. All of the prepared samples exhibited the typical fracture behavior of highly porous ceramic scaffolds [44] regardless of the initial BCP content. In detail, a steady increase in compressive stress with an elastic response was observed in primary stage, followed by rapid decrease due to fast fracture of the BCP walls. Increase of an initial BCP content from 15 to 25 vol% showed higher compressive strength from 16.1 ± 1.5 up to 19.3 ± 2.7 MPa. In addition, compression strength of the samples with heat treatment was much higher than that of the samples without heat treatment, as shown in Fig 1.14. This suggests that the heat treatment at 33°C attributed to the continuous overgrowth of camphene dendrites without sacrificing or disturbing the aligned structure formed during the extrusion process. Moreover, the structural integrity of samples strongly affects the mechanical properties of the porous ceramic. It should be noted that scaffolds with controlled pore structure, bioactive environment, and sufficient mechanical properties need to be balanced to be applied in tissue engineering [45]. Table 1.3 summarizes the compressive strength of the porous tubular BCP scaffold, which loads were applied in parallel direction of pore alignment. Compared to those of cylindrical scaffolds, mechanical strength were slightly higher due to central region which was formed as a replica of camphene rod. In addition, the

effect of the post-treatment time on the compressive strengths of the porous BCP scaffolds was reconfirmed by compressive tests on multi-channeled BCP samples with initial BCP content of 15 vol% (Table 1.4). Interestingly, the compressive strength of the samples was relatively higher than those of tubular samples. This result is attributed by the difference in actual reduction ratio, resulting in more densificated BCP walls. This suggests that complex shape of porous ceramic could be produced simply by assembling unidirectionally frozen BCP/camphene bodies without sacrificing the unique properties. And owing to the preservation of the aligned pore structure, enhanced mechanical properties could be provided.

However, it is still necessary to design porous bioceramics with controlled pore structure that include the necessary mechanical properties to ensure its clinical application. So in following part 2, we reported the study about the hybrid solution and composite which could be used as coating solution for porous BCP scaffolds to overcome the limitation of the scaffold strength, of which the main purpose of part 3.

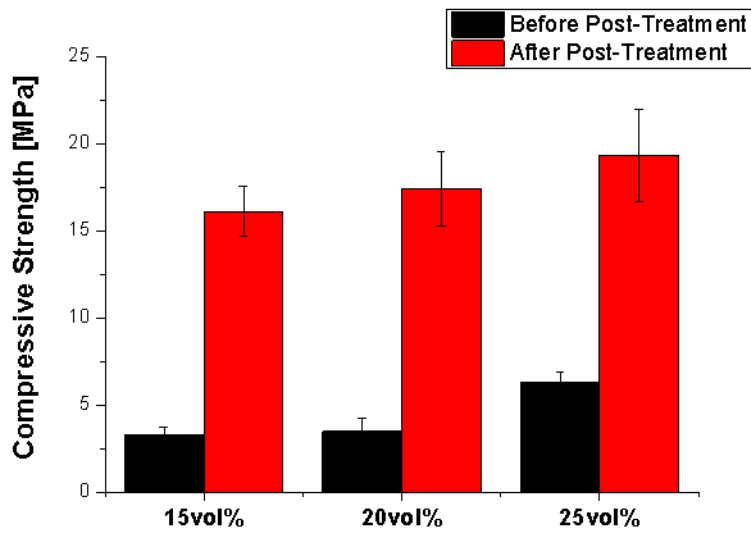
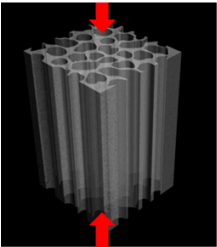


Figure 1.14 Compressive strengths of the porous cylindrical BCP scaffolds with BCP contents of 15, 20, and 25vol%, before and after post-treatment.

Table 1.3 Compressive strengths of the porous tubular BCP scaffolds with BCP contents of 15, 20, and 25vol%, before and after post-treatment.

Compressive Strength (MPa)		
BCP Content	Before Post-Treatment	After Post-Treatment
15 vol%	9.2 ± 0.9	17.6 ± 2.9
20 vol%	10.8 ± 1.3	20.8 ± 2.4
25 vol%	12.4 ± 1.6	24.3 ± 4.2

Table 1.4 Compressive strengths of the multi-channeled porous BCP scaffolds with initial BCP contents of 15 vol%.



Post-Treatment Time	Compressive Strength [Mpa]
0h	19.4 ± 4.0
1h	25.0 ± 4.6
6h	28.4 ± 7.8
12h	33.0 ± 4.4
24h	37.1 ± 6.8

Cellular Responses

A variety of calcium phosphates have been used for bone engineering applications due to osteoconductive nature which allows new bone formation. In case of BCP (biphasic calcium phosphate), have the benefits of combining the reactivity of β -TCP and the stability of HA^[37]. With the aim of good biocompatibility and bioactivity, preliminary osteoblastic activity of the samples was evaluated by *in vitro* cell test in terms of initial cell attachment of MC3T3-E1 cells. Fig 1.15 (A)-(C) show typical SEM images of the MC3T3 cells attached to the porous BCP scaffolds with various BCP contents (15, 20, and 25 vol%) after 1 day of culturing. All of the produced scaffolds showed that the cells adhered and spread actively on their surfaces regardless of initial BCP content, indicating that porous BCP scaffolds with aligned pore structure produced in this study have good *in vitro* biocompatibility.

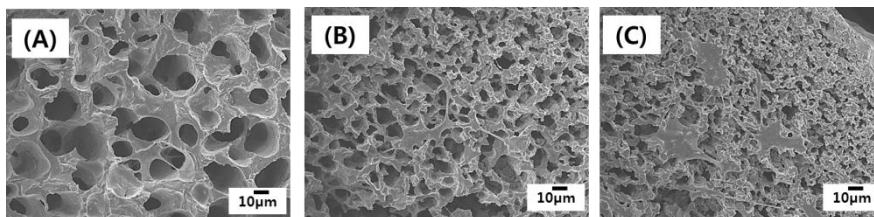


Figure 1.15 Typical SEM images of the cells cultured for 1day on the porous BCP scaffolds with BCP contents of (A) 15, (B) 20, and (C) 25vol%.

4. Conclusions

Extruding frozen BCP/camphene body was used to produce porous BCP ceramic with aligned pores, followed by freeze drying and sintering to densify BCP walls. Extensive deformation and elongation of the camphene dendrite was attributed to extrusion process, which formed interconnected and unidirectionally aligned pores by removal of camphene. The pore structure and porosities of the samples were tailored by adjusting the initial BCP content in the BCP/camphene slurry and post-treatment at 33°C, which is close to solidification temperature of camphene. In addition, the mechanical strength were enhanced as increase of initial BCP content. Diverse designs such as cylindrical, tubular, and multi-channeled type of the scaffold were fabricated and evaluated. These porous BCP scaffold prepared in the study are expected to applicable in bone tissue engineering.

Part II.

PCL-based Hybrid Scaffold
: Hybrid Coating Materials for Efficient BMP
Loading

1. Introduction

Porous polymeric scaffolds are widely used in tissue engineering as a support template for cellular attachment, growth, and tissue regeneration. Studies on natural, synthetic, and combinations of both materials as biocompatible, biodegradable polymeric matrix and hybridization with bioactive inorganic materials have been reported with great interests⁴⁶⁴⁷⁴⁸⁴⁹⁵⁰⁵¹. Porous polymeric membranes are one of the most desirable forms in tissue engineering^[5253], which can not only stimulate the cell viability by pore structure control, but also potential application as a carrier^[54]. Studies on the development of the porous membranes have been reported with great interests^[555657]. In addition, appropriate mechanical strength is needed to sustain loads as tissues grow^[5859].

Among those biopolymers used as a matrix, polycaprolactone is one of the most widely used biodegradable and bioresorbable polymers, which has been extensively studied owing to its flexibility, great mechanical properties, biocompatibility^[6061], and biodegradability^[62636465]. However, pure PCL has limitation, as other synthetic biopolymers, such as relatively low stiffness, cell adhesion, and hydrophilicity^[66]. Therefore, there have been considerable efforts to hybridize PCL polymer with bioactive inorganic materials, such as calcium phosphate⁶⁷⁶⁸ and bioactive glass⁶⁹, with the aim of not only increasing the bioactivity, but also enhancing the mechanical properties of the scaffold⁷⁰⁷¹, on account of improved stiffness and cell viability compared with their individual components ^[7273].

Recently, there has been a particular interest in the synthesis of

bioactive silica by the sol-gel process, which can be fabricated at room temperature with similar atomic composition as that of bioactive glass^[7475]. Sol-gel derived silica has significant advantages, such as uniform size dispersion, possibility of fine control of composition in hybridization, relatively cheap, and simplicity ^[76 77]. Moreover, they also have a mesoporous structure, which is suitable for encapsulating bioactive agents such as drugs, proteins, and growth factors^[78]. Therefore, silica synthesized by sol-gel method is one of a strong candidate as an inorganic material for hybridization with biopolymer^[7980]

The objective of this study was to produce a porous polycaprolactone/sol-gel derived silica hybrid with controlled pore structure by solvent casting for potential material as drug eluting membrane. The membranes with different silica contents up to 30vol% were prepared by casting a mixture of a PCL and sol-gel derived silica sol. The use of a silica phase in PCL matrix would allow the improvement in aspect of mechanical properties, bioactivities, and biomolecule-carrying potential. Pore network and porous structure of the membranes were characterized and the chemical composition, drug release profile were examined by Fourier transform infrared spectroscopy and UV spectrometer, respectively.

2. Experimental Procedure

Fabrication of PCL/sol-gel derived silica membrane

In this study we propose a novel way of producing porous poly(ϵ -caprolactone)/silica hybrid membranes with controlled pore structure by casting a mixture of a PCL solution and sol-gel derived silica sol. First, a poly(ϵ -caprolactone) solution was prepared by dissolving 8 g PCL (Sigma Aldrich, USA, Mn=70,000~90,000) in a mixture containing 30 mL of dichloroethane(DCE, Sigma Aldrich, USA) and 10 mL of N, N-dimethylformamide(DMF, Sigma Aldrich, USA) as the solvent and non-solvent, respectively^[67]. In a separate preparation, the silica sol was synthesized using a sol gel process at room temperature by mixing tetraethyl orthosilicate(TEOS, $\text{Si}(\text{OC}_2\text{H}_5)_4$), distilled water, and ethanol at a molar ratio of 1:2:1 with 1N HCl as a catalyst using a magnetic stirrer for 2 h. Prepared silica sol was added with various amounts, namely, initial TEOS contents of 0, 10, 20, and 30 vol% in relation to the PCL content. In addition, tetracycline hydrate(TCH, Sigma-Aldrich, USA) and growth factor were added to TEOS solution and stirred for 6 hours in room temperature to achieve homogeneous dispersion. The mixture was magnetically stirred for 24 h at room temperature, then cast into glass Petri dishes and dried at room temperature for more than 12 h.

Characterization

The microstructure of the hybrid membranes was examined by field emission scanning electron microscopy (FESEM; JSM-6701F, JEOL, Japan).

The pore sizes of the membranes were measured and averaged roughly from SEM images. The porosity was also calculated by considering the final content of the silica phase in the hybrid membrane and the density of the sample. The silica distribution in the hybrids was analyzed with energy dispersive spectroscopy (EDS) connected to the FESEM. The internal organized structure of the hybrids was examined by high-resolution transmission electron microscopy (HR-TEM, JEM-3010, JEOL, Tokyo, Japan). A drop of the hybrid solution was placed onto a carbon coated grid.

GFP was used for the visualization of the membrane containing the growth factor. The surface of the membrane before and after BMP addition was observed by confocal laser scanning microscopy (CLSM, Olympus Fluoview 100, Olympus, Tokyo, Japan).

Mechanical Tests

For the purpose of mechanical tests, tensile tests were performed in accordance of screw driven load frame (Oriental testing machine, Korea). The samples with dimensions of $\sim 0.09 \times 7 \times 15$ mm were loaded at a stretching speed of 5 mm/min using a screw driven load frame (Oriental testing machine, Korea). The tensile strength, elastic modulus, and strain at failure were calculated from the stress-strain curves obtained from each test. Five samples were tested to calculate the average value and standard deviation.

Antibiotic Release Behavior

The specimens were immersed in 10ml of PBS for over 250 hours in

vials, incubated at 37°C to analyze tetracycline release behaviors. Half of the medium was taken at predetermined periods of time and the concentration of TCH was analyzed by measuring the absorbance at 355 nm using UV spectrometer (V-60, JASCO, Japan). An equivalent amount of new PBS was replaced to the incubation solutions. The released amount of TCH was determined from an absorbance-concentration standard curve, which was drawn from the absorbance of the 0.4 to 70 µg of TCH dissolved in the PBS 10ml

Cellular Responses

The biological properties were assessed by proliferation and differentiation behavior of the MC3T3-E1 cell line (ATCC, CRL-2593). Prior to seeding cells, the samples were sterilized with 90% ethanol and then dried on a clean bench under ultraviolet (UV) irradiation for 12 hours. For the proliferation and differentiation tests, cells were cultured in a humidified incubator in an atmosphere containing 5% CO₂ at 37°C. The proliferation behavior was examined by using MTS (methoxyphenyl tetrazolium salt) method. The culture medium was removed and the specimens were rinsed with PBS solution after culturing for 5 days. The absorbance of specimens was measured at 490 nm using a micro-reader (Biorad, Model 550, USA). The degrees of cell differentiation were analyzed by alkaline phosphatase (ALP) activity. The ALP activity was measured as an early marker of the maintenance of the osteoblastic phenotype using p-nitrophenyl phosphate (pNPP) (Sigma-Aldrich, UK), after culturing for 14 days. The ALP activity

levels were calculated from a standard curve obtained with bovine serum albumin. The production of pNP was determined by the absorbance at 405 nm measured using a microreader. All experiments were performed three times with results collected from triplicate samples ($n = 3$), statistical analysis was carried out using one-way analysis of variance with statistical significance at $p < 0.01(*)$.

3. Results and discussion

Poly(ϵ -caprolactone)/silica hybrid membranes with controlled pore structure were fabricated by casting a mixture of a PCL solution and sol-gel derived silica sol. Fundamentally, the morphology of the polymeric membranes prepared by solvent casting should be strongly affected by the type and amount of solvent and/or non-solvent used to dissolve the polymer [81]. In this research, dichloroethane and dimethylformamide were used as solvent and non-solvent, respectively, and prepared solution was consisted of 75vol% of DCE and 25vol% of DMF. The mechanism of the formation of a porous structure of the membrane is still unclear, however, it is believed that the nonsolvents (DMF, ethanol, and water) for the PCL polymer play a key role in the formation of porous hybrid membranes[82]. After solvent casting, DCE, the solvent for the PCL polymer, evaporated faster than any other liquid used in this work due to high vapor pressure. As consequence, the PCL phase solidifies with hybridization with the silica phase, and the other remaining DMF, distilled water, and ethanol would be forced to move to the liquid phase. They would form spherical shapes and float to the surface of the hybrid membrane, resulting in large patterned pores with small internal pores.

Microstructure and Structural properties

The microstructure of the hybrid membranes were observed by scanning electron microscopy as shown in Figs. 2.1. The porous structure of the hybrid membranes were strongly affected by the initial TEOS contents in

relation to PCL content. The membrane of pure PCL without a TEOS showed relatively dense structure from the observation by SEM. However, the increase of silica content from 10 to 20 vol% resulted in more porous structure. The pore structure (i.e. pore size and porosity) is known as major factors affecting the properties of porous scaffold, in the tissue engineering applications^[39, 83]. The size of pores in the hybrid membranes prepared with an initial TEOS content of 0, 10, 20, and 30 vol.% was 10.5 ± 2.4 , 3.6 ± 0.5 , 8.3 ± 1.6 , and 12.7 ± 0.8 μm , respectively, as shown in Fig 2.2. (A). The porosity was estimated by considering the final content of PCL and silica phase in the membrane, and theoretical densities of PCL 1.1 and sol-gel derived silica 1.9g/cm³, respectively. The porosity was increased from 6.8 to 33.9% with the increase of initial TEOS content (Fig. 2.2.(B)). This is presumably attributed to increased sol-gel derived silica phase in the membrane, which has intrinsic mesoporous structure.

The nanostructural organization of the PCL/silica hybrid membrane was observed by TEM. Sol-gel derived silica was well-dispersed in PCL matrix with mesoporous structure, as shown in Fig 2.3. EDS mapping of the PCL/silica membrane showed that the silica phases were well-dispersed in the PCL matrix without noticeable agglomerations (Fig 2.4). These result revealed that the silica was synthesized and dispersed homogeneously in the PCL matrix to form a hybrid membrane through a sol-gel process.

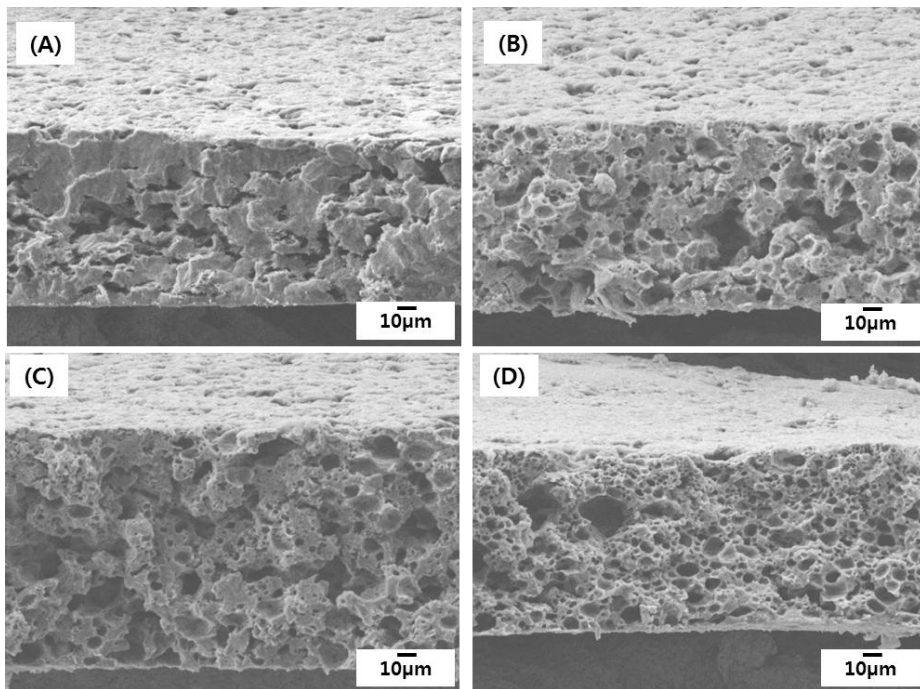


Figure 2.1. Cross-sectional SEM images of the porous PCL/sol-gel derived silica membranes produced with various initial TEOS contents (A) 0, (B) 10, (C) 20, and (D) 30 vol%.

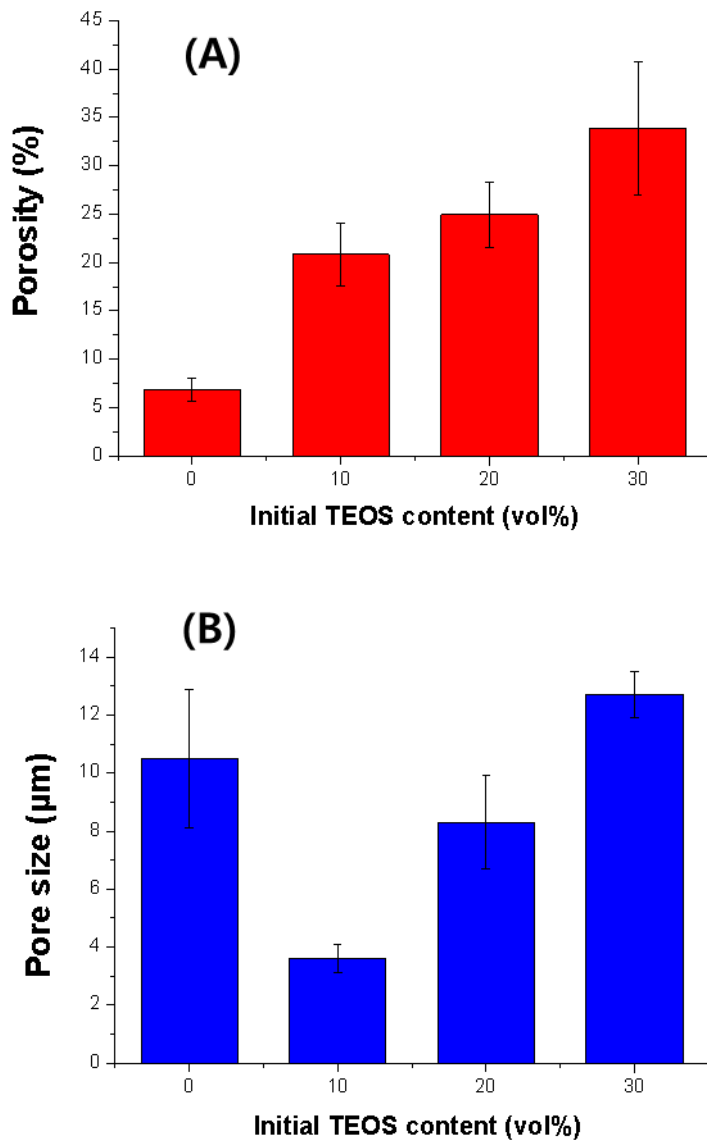


Figure 2.2. Porosity and pore size of the porous PCL/sol-gel derived silica membranes produced with various initial TEOS contents

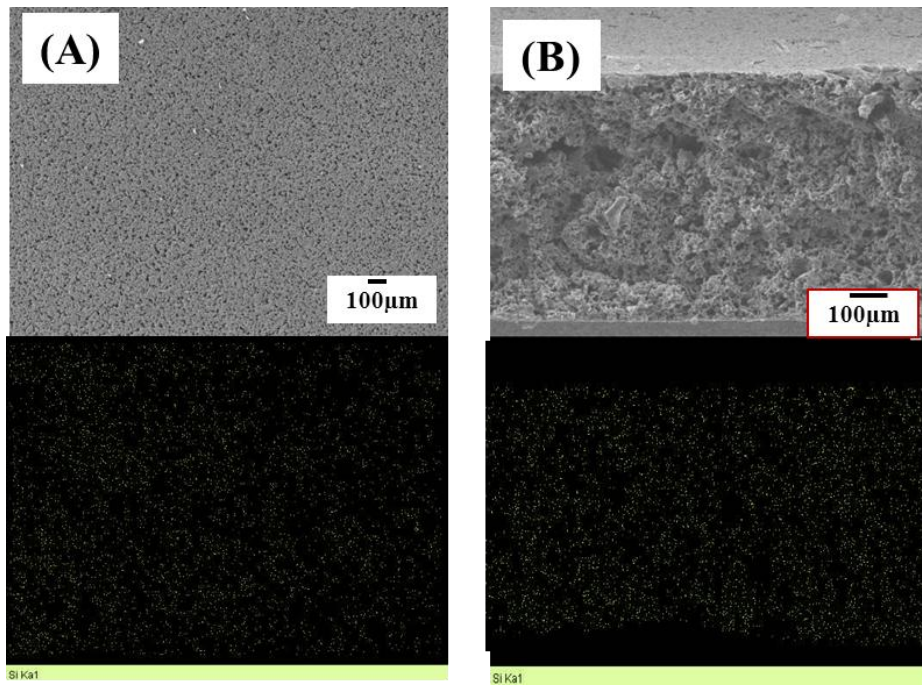


Figure 2.3. EDS analysis of the porous PCL/silica hybrid membranes of (A) surface and (B) cross-section.

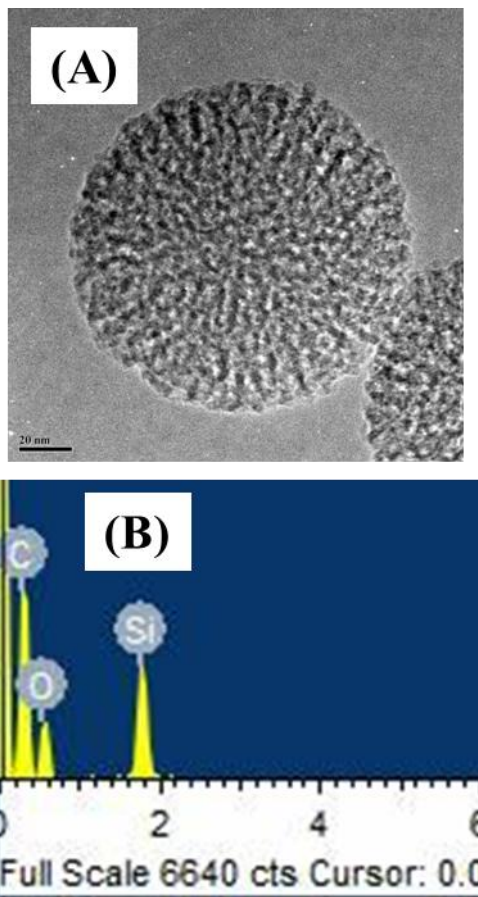


Figure 2.4. (A) TEM images and (B) EDS analysis of the porous PCL/silica hybrid membranes.

Chemical Structure

The chemical structure of the hybrid membranes with and without antibiotics was examined by Fourier transform infrared spectroscopy as shown in Fig 2.5. Typical characteristic bands of the PCL polymer were shown at 1750 and 1180 cm^{-1} , corresponding to the stretching vibrations of carboxyl(C-O) and ether groups (C-O-C)[^{84 85}], respectively. Several characteristic bands of sol-gel derived silica were observed in the spectra at approximately 1078 and 795 cm^{-1} , which are the representative of the various vibration modes of the Si-O-Si bonds and a band at approximately 938 cm^{-1} , assigned to Si-OH stretching vibrations. No noticeable band shift was observed in all of the membranes, suggesting that the intrinsic characteristics of the PCL polymer and silica phase were preserved.

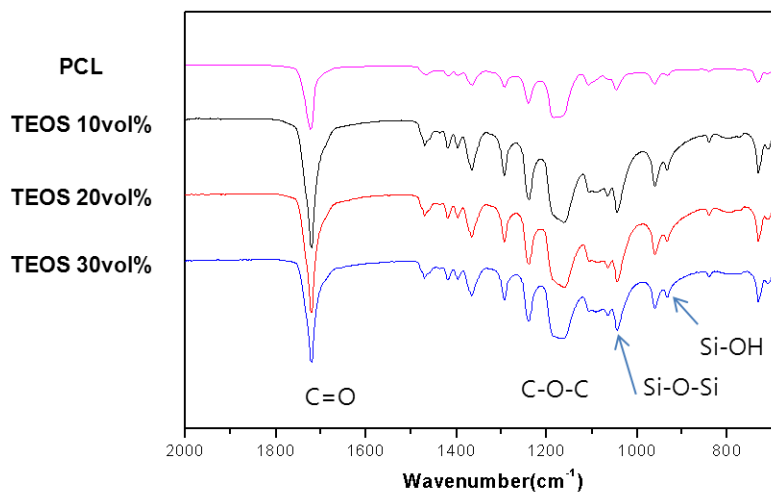


Figure 2.5 Chemical composition of the porous PCL/sol-gel derived silica membranes produced with various initial TEOS contents(0, 10, 20, and 30vol%), by FT-IR

Hydrophilicity

The attachment and growth of cells need materials with a hydrophilic surface [8687]. Cell affinity in terms of adhesion spreading and migration is influenced by the surface charge, morphology and hydrophilicity of the hybrid membrane. Recent researches reported that a hydrophilic surface improves cell affinity[88]. In the wettability tests, the PCL membranes had the contact angles of $81.6 \pm 3.2^\circ$, which indicates a hydrophobic material. The contact angles of hybridized membranes with silica phase decreased to 75.9 ± 2.7 , 72.3 ± 2.2 , $69.8 \pm 2.5^\circ$ as the initial TEOS content increased (Fig 2.6). It should be noted that hydrophilicity of the materials are strongly affected by not only the hydrophilic nature, but also the surface roughness of the materials. The surface of the membranes was observed by SEM, as shown in Fig 2.6. The pore sizes on the surface increased from 43 ± 4.7 to $67 \pm 8.8\mu\text{m}$. This results indicate that the larger pores on the surface and hydrophilic character of silica phase improved the hydrophilicity of the membranes[89], which would attribute to the results of cell culture.

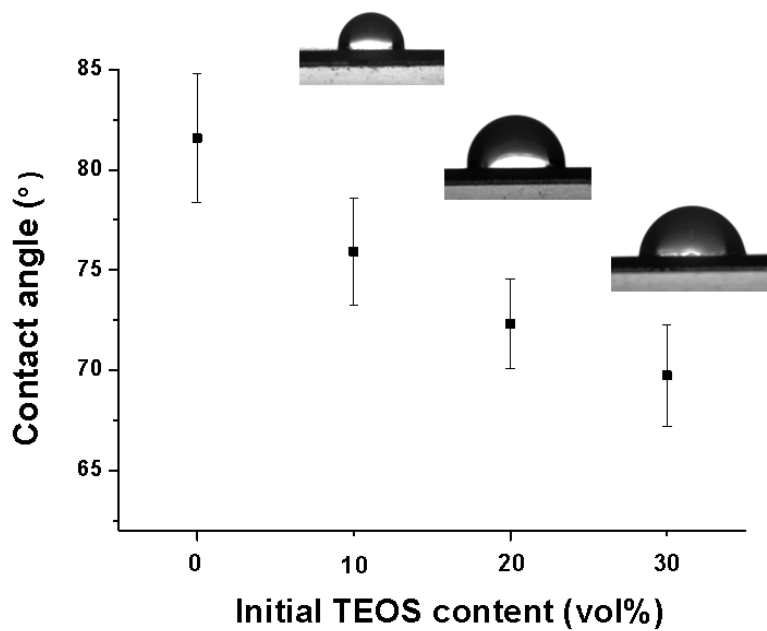


Figure 2.6. Water contact angle of the porous PCL/sol-gel derived silica membranes produced with various initial TEOS contents

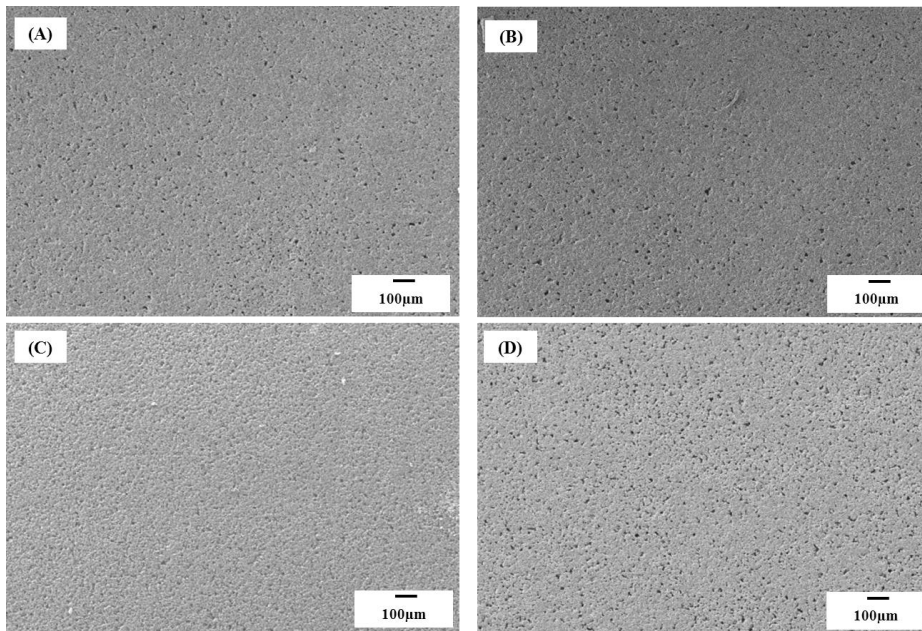


Figure 2.7. Surface SEM images of the porous PCL/sol-gel derived silica membranes produced with various initial TEOS contents (A) 0, (B) 10, (C) 20, and (D) 30 vol%.

Drug Release Behavior

The effect of silica content on the TCH release behavior of the porous PCL/silica membrane investigated in PBS solution up to 250 hours with encapsulation of 1mg/ml of TCH. Fig 2.8 presents the cumulative amount of TCH released from the prepared hybrid membranes with an equal amount of TCH loading relative to the amount of the drug initially loaded. The hybrid membranes were more effective in releasing the drugs apparently than that of PCL membrane. About 30% of loaded TCH was released within 15 hours of immersion for all samples, which would be the abrupt release of the exposed drug on the surface of the membrane. After initial release stage, the TCH release rate slowed down via diffusion of the entrapped drug in between porous network. In this region, the slopes of release rate were similar regardless of initial TEOS content, implying that the release profile is not only affected by the component of the membrane but also the inner pore network. The release rate was very slow after 120 hour period. The release rate during this period was observed to be in the order of increasing initial TEOS content, clearly indicating a decreasing TCH release rate with increasing silica content.

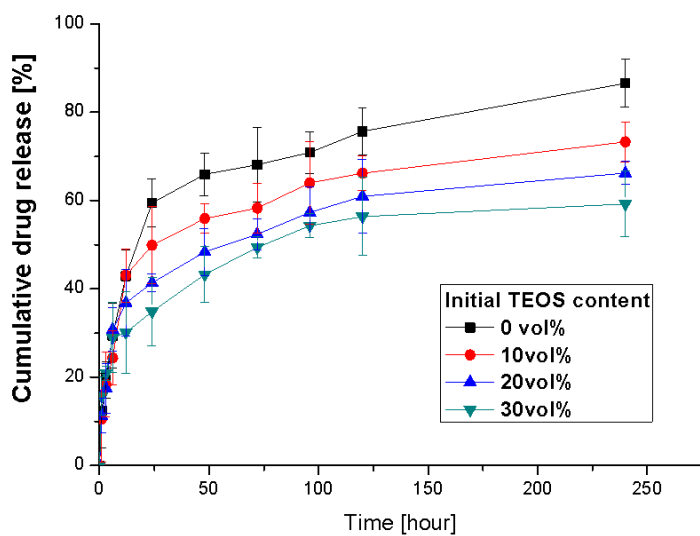


Figure 2.8. Cumulative drug release of the porous PCL/sol-gel derived silica membranes produced with various initial TEOS contents

Loading capability of growth factor

The presence of the growth factor in the hybrid membrane was confirmed by CLSM using GFP, as shown in Fig 2.9. The green fluorescence of the growth factor visualized the incorporation of growth factor. It could be observed from CLSM micrograph that the hybrid membrane containing BMP was uniformly covered regardless of conditions of membrane.

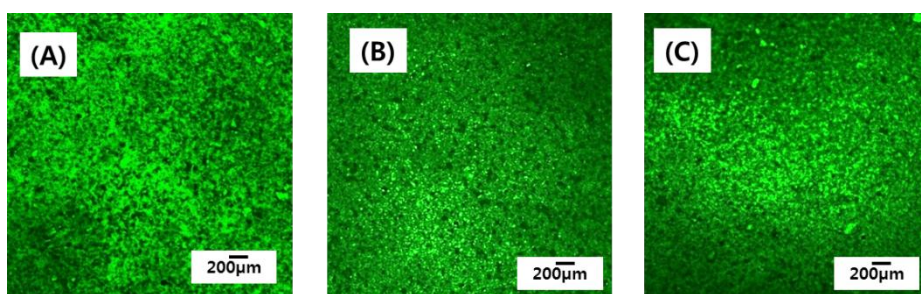


Figure 2.9. CLSM Visualization of the growth factor by green fluorescence with various initial TEOS contents, (A) 10, (B) 20, and (C) 30vol%

Cellular Responses

The biocompatibility of the PCL/silica hybrid membranes was assessed by *in vitro* cell tests in terms of proliferation, and differentiation of MC3T3-E1 cells. Improved cell proliferation and differentiation were observed as compared with the pure PCL. Fig. 2.10 shows the degree of cell proliferation determined by the MTS method cultured for 5 days and the level of osteoblastic differentiation of the MC3T3-E1 cells by measuring the ALP activity after 14 days. With the increasing initial TEOS content, higher levels of cell viability was appeared, compared with that of the pure PCL membrane. The proliferation and differentiation increased with increasing silica content from 0 to 30 vol%, suggesting that the presence of the silica phase would be highly beneficial to the expression of the osteoblastic phenotype. These results indicate that the biocompatibility of the membranes was enhanced by the hybridization with silica phase. Compared with the PCL control, the PCL/silica membrane is considered to have great potential for use as a tissue regenerative field.

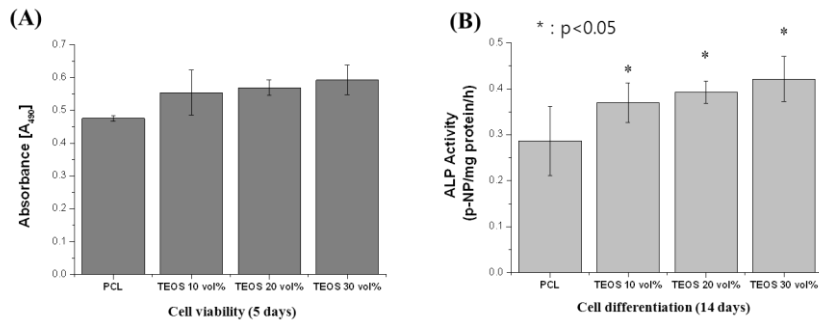


Figure 2.10 (A) Viability of the cells on the membrane after culturing for up to 5 days, (B) alkaline phosphatase activity(ALP) of the MC3T3 cells

4. Conclusions

This study reports the novel method of fabrication of the porous PCL/sol-gel derived silica hybrid membrane with controlled pore structure using solvent casting. The hybrids were fabricated by casting a mixture of a PCL/DCE/DMF solution and sol-gel derived silica sol. The membranes with a various initial TEOS contents in the relation to the PCL contents(0, 10, 20, and 30vol%) in the mixture were prepared. TCH was loaded as drug and release behavior was examined for potential application as drug eluting membrane. The silica phase was hybridized uniformly with the PCL phase, and the porous structures were strongly affected by the initial TEOS contents in relation to PCL in the mixture. The hybridization of the PCL polymer with silica phase increased the stiffness and biocompatibility of the membrane with respect to that of pure PCL.

Part III.

GF/Drug-releasing Intelligent Hybrid Scaffold

: BCP/(PCL-Silica) Hybrid Scaffold

1. Introduction

Bone tissue engineering requires three-dimensional matrix, to act as a scaffold for cell adhesion and proliferation, with adequate strength to be used as a supporting framework that can sustain loads as tissues grow [32]. There are some requirements for the ideal scaffold, such as interconnected pore network, biocompatible surface for cells to attach and grow, biodegradable, adequate mechanical properties, and three-dimensional matrix [90]. To date, a number of materials have received a particular interest as potential scaffold for bone tissue engineering, as summarized in Fig 3.1.1[96]. Among these materials, bioceramics has been widely studied in bone tissue engineering field because of their osteoconductive properties and similar chemical composition to human bone, mainly calcium phosphate and bioactive glass[9192]. However, bioceramic has limitations to be applied in a wide range of field, since they possess brittle fracture behavior. Therefore considerable efforts have been made to improve the mechanical properties of bioceramics. Combining bioceramics with polymer would be the one of the solution. In particular, coating of their surfaces with biopolymer solution can be one of the solutions to improve the mechanical properties, while preserving the biocompatible environment for bone cells to attach and grow with addition of inorganic compound to the biopolymer solution.

Carrier	Benefits	Potential Issues	Types
Inorganic materials	Similar structure to bone (calcium phosphates) Resorbable or non-resorbable Affinity for BMP's	Brittle Difficult to mold Exothermic (some CaP cements)	Porous coralline hydroxyapatite, β -TCP, hyaluronic acid, calcium phosphate cements, metals and calcium sulfate
Synthetic polymers	Reproducible manufacture Readily tailored controlled release properties Ease of sterilization	Break-down products might be inflammatory Synthetic materials and cell recognition Solvents or crosslinkers might denature proteins	Poly(α -hydroxy acids), polypropylene fumarate, polyanhydrides, polyphosphazenes, polyethylene glycol
Naturally-derived polymers	Excellent biocompatibility May have natural affinity for growth factors	Pathogen transmission, sterilization	Fibrin glue, collagen, chitosan and hyaluronic acid
Composite materials	Benefits from different materials exploited	More complex manufacturing process	Collagen-TCP, collagen-HA and TCP-cellulose

Table 3.1. Major classes of materials used as scaffold for bone growth factor [96]

Based on these considerations, the development of the biomaterial for bone tissue engineering should be mainly focused on the scaffolds with three-dimensionally interconnected pore network, adequate pore size, biocompatible surface and environment, and biodegradable with sufficient mechanical properties. Therefore in this work, coating the porous bioceramic scaffold with biopolymer/inorganic solution is proposed.

As mentioned above, since hydroxyapatite-based calcium phosphate is considered as a strong candidate material in bone tissue engineering, we have produced porous biphasic calcium phosphate ceramic by extruding a frozen BCP/camphene body to control the pore structure in part I. Also, we have studied hybrid materials composed of PCL as biopolymer and silica as the inorganic phase. Especially, hybridizing PCL with sol-gel derived silica showed the capability of encapsulation of antibiotics or growth factor, as reported in Part II. Human bone contains a reservoir of bone-building cells(osteoblasts), which deposit from extracellular matrix(ECM) and convert into mineralized hard tissue. This bone contains a group of growth factors including transforming growth factor beta(TGF- β), platelet-derived growth factor(PDGF), fibroblast growth factor(FGF), insulin-like growth factor(IGF), and bone morphogenetic protein(BMP)(Fig 3.1.2.[⁹³]). So in part III, for biomimicking human bone, we propose a simple, novel way of fabricating porous BCP/PCL/silica scaffold with encapsulate growth factor, BMP in this study, for potential material for bone tissue engineering, based on the results of part I and II. Coating of the porous BCP scaffold with biopolymer /inorganic phase solution can be a candidate to improve the mechanical

properties, while preserving the biocompatible environment for bone cells to attach and grow. For their potential use as scaffold, the examinations on pore structure, coating capability, and mechanical properties were performed. The release behavior of growth factor, in vitro cellular responses, and in vivo animal tests were assessed.

Growth Factor	Source	Receptor Class	Function
Transforming growth factor beta (TGF- β)	Platelets, bone extracellular matrix, cartilage matrix	Serine threonine sulfate	Pleiotropic growth factor stimulates undifferentiated mesenchymal cell proliferation
Bone morphogenetic protein (BMP)	Osteoprogenitor cells, osteoblasts, bone extracellular matrix	Serine threonine sulfate	Promotes differentiation of mesenchymal cells into chondrocytes and osteoblasts, promotes differentiation of osteoprogenitors into osteoblasts, influences skeletal pattern formation
Fibroblast growth factors (FGF)	Macrophages, mesenchymal cells, chondrocytes, osteoblasts	Tyrosine kinase	Mitogenic for mesenchymal cells, chondrocytes, and osteoblasts
Insulin-like growth factors (IGF)	Bone matrix, osteoblasts, chondrocytes	Tyrosine kinase	Promotes proliferation and differentiation of osteoprogenitor cells
Platelet-derived growth factor (PDGF)	Platelets, osteoblasts	Tyrosine kinase	Mitogen for mesenchymal cells and osteoblasts; macrophage chemotaxis

Table 3.2. Types of growth factors [93]

2. Experimental Procedure

Preparation of porous BCP ceramic scaffold

Porous tubular BCP ceramic scaffold was fabricated by same method mentioned in part I. In brief, aligned porous BCP scaffolds with an initial BCP content of 15,20, and 25vol% were fabricated by ball-milling, freeze casting, freeze drying, and sintering. The assembled frozen BCP/camphene body and camphene rod was extruded through a reduction die with an orifice of 3mm diameter, which attributed to the preferential orientation of camphene dendrite along the direction of extrusion. Subsequently, the extruded green bodies were post-treated at 33 °C for 3 hours in oven, and then placed in freeze dryer remove the solid camphene by sublimation for 24 hours. Freeze dried samples were then sintered at 1250 °C for 3 hours to densify the BCP walls.

For coating solution, poly(ϵ -caprolactone)/sol-gel derived silica/growth factor(bone morphogenetic protein, BMP-2) solution was prepared, as mentioned in part II. PCL/DCE/DMF solution and the silica sol with growth factor were mixed with an initial TEOS content of 10 vol% in relation to the PCL content. The mixture was magnetically stirred for 24 h at room temperature, then porous BCP ceramic scaffolds were dip-coated under reduced pressure, in the range of 50-70 kPa, which allowed the removal of air bubbles in the scaffolds.

Characterization

The pore structures of the fabricated samples were characterized by

field emission scanning electron microscopy(FE-SEM, JSM-67010F, JEOL, Japan). Porosity, pore size, degree of pore alignment, pore interconnection, and microstructure of coated body were observed.

Mechanical Tests

For the purpose of mechanical tests, compression strength test was performed in accordance of screw driven load frame (OTU-05D, Oriental TM Corp., Korea). The samples with dimensions of ϕ 3mm x ~ 6mm were compressed parallel to the direction of pore alignment, loaded at a pressing speed of 1 mm/min and load-extension data were obtained from six samples and used to calculate an average value and its standard deviation of compressive strength.

In Vitro Release

The samples were immersed in 10ml of PBS for over 24 days in vials, incubated at 37°C to analyze BMP-2 release behaviors. Half of the medium was taken at predetermined periods of time and the concentration of BMP-2 was analyzed by measuring the absorbance at 198 nm using UV spectrometer (V-630, JASCO, Japan). An equivalent amount of new PBS was replaced to the incubation solutions. The released amount of BMP-2 was calculated using the absorbance(x) and BMP concentration(y).

In Vitro Cellular Tests

For the examination of its biological properties, in vitro cell tests of

the porous BCP/PCL/silica hybrid scaffolds were assessed by attachment, proliferation, and differentiation behavior of the MC3T3-E1 cell line (ATCC, CRL-2593, Rockville, MD). The cell attachment was observed by CLSM, proliferation behavior by using MTS (methoxyphenyl tetrazolium salt) method, and the degrees of cell differentiation by alkaline phosphatase (ALP) activity, respectively. All experiments were performed three times with results collected from triplicate samples ($n = 3$), statistical analysis was carried out using one-way analysis of variance with statistical significance at $p < 0.01$ (*).

In vivo animal test

For the *in vivo* test, the porous hybrid BCP scaffold with a diameter of 2.9mm, and length of 5mm were prepared. To compare the osseointegration of the scaffold, bare BCP scaffold and hybridized only with PCL/silica solution were prepared. Twelve skeletal mature Sprague Dawley rats (male, 6weeks, body weight 300-400g) were anesthetized by intraperitoneal injection of Tiletamine/Zolazepam (0.025 mL/100 g, Zoletil® 50, Virbac Laboratories, France), Xylazine(0.025 mL/100 g, Rompun® 2%, Bayer Healthcare Korea,Korea). The housing care and experimental protocol were approved by the Institutional Animal Care and Use Committee of the University of Korea Medical Center (Seoul, Korea; KUIACUC-2010 – 113). The right legs of rat were shaved and prepared for sterile isolation. A 2-cm skin incision was made over the medial aspect of right proximal tibia. The perisoteum and soft tissue carefully retracted, and the tibia was exposed.

Four 0.9 mm k-wires (Zimmer® , Warsaw, IN) were used to drill both cortices of the tibia. K-wires were clamped bilaterally with author own designed external fixator (U&I, Kyunggido, Korea). The tibia was osteotomized between second and third k-wire. The osteotomized gap was compressed using the external fixator. Subcutaneous tissue and skin was sutured. The animals were allowed free movement in cages after recovery from anesthesia. After operation, the radiographs were taken with certain time interval. The progress of bone formation was determined by radiographic X-ray analysis(Image Station, DXS 4000MM PRO, Carestream, USA). On the post-operative day and 4 weeks after the operation, anteroposterior and lateral plane radiographs were taken under peritoneal anesthesia to assess the progression of bone union, loss of correction, fixation, failure and collapse of osteotomy site on serial plane radiographs. The bones were placed on a customized platform(FOV 80 Chamber), an X-ray tube (RFM-525HF) positioned 100 cm from the bone, and lateral radiographs obtained using iCR 1000. The setting for the machine was 35 kV and 50 mA, with a 30s exposure time.

3. Results and discussion

Microstructure Observation

Fig 3.1 shows the microstructure of the samples coated with PCL/silica/BMP-2 mixture. All of the prepared samples showed successful coating of mixture without severe defects such as agglomeration or sedimentation. Even though the pore size decreased as the BCP content increased, PCL/silica/BMP-2 mixture was well-loaded to the porous BCP scaffolds. The fracture surface of the samples also shows proper loading of the mixture (Fig 3.2.(A)(B)). Regardless of the pore size of the porous BCP scaffolds, the mixture covered ceramics homogenously by dip-coating. Without vacuum process, trapped air bubbles were observed in the fracture surface and delamination of the coating layer was found on the surface(Fig 3.2.(C)).

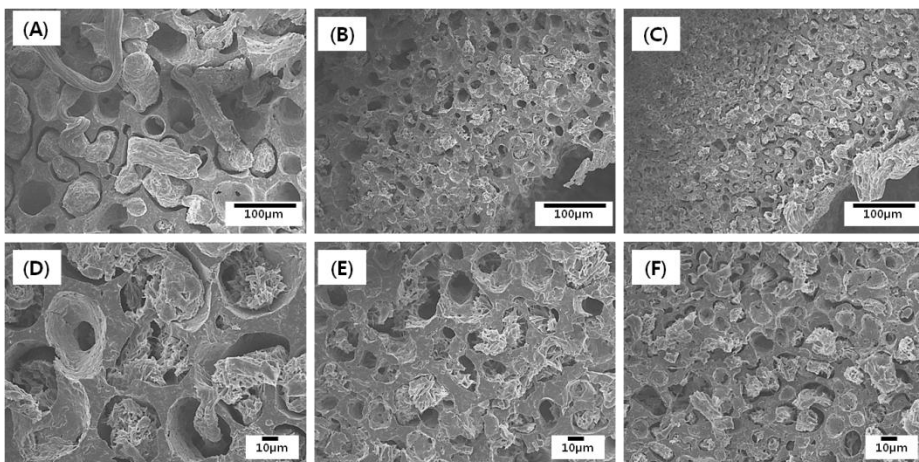


Figure 3.1. Representative SEM images of the porous BCP scaffolds coated with hybrid solution with BCP contents of (A)(D) 15, (B)(E) 20, and (C)(F) 25 vol%, showing infiltration of the hybrid solution.

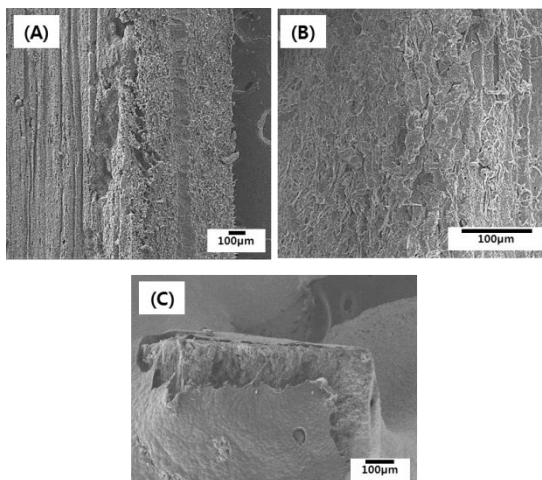


Figure 3.2. Representative SEM images of the porous BCP scaffolds coated with hybrid solution with BCP contents of 15vol%, showing coating of the hybrid solution.

Mechanical Properties

In order to examine the effect of the hybrid coating on the mechanical properties of the aligned porous BCP scaffolds, compressive strength tests were carried out. Loads were applied in parallel direction of pore alignment in compressive strength test. All of the hybrid loaded samples exhibited the retained fracture behavior, of which polymeric coating layer absorbed the cracked ceramic phase, consequently toughening of the scaffold, as summarized in Fig 3.3. The fractured ceramic phases were entrapped in polymeric coating layer and densified as loads were applied. In detail, a steady increase in compressive stress with an elastic response was observed in primary stage, followed by gradual decrease due to polymeric coating layer. After coating with hybrid solution, compressive strengths were increased compared to those of the bare BCP scaffolds. For comparison, human cancellous bone has a compressive strength of 4–12 MPa^[94]. These results also indicate that the structural integrity of samples strongly affects the mechanical properties of the porous scaffold, and the prepared hybrid-loaded BCP scaffolds have potential to be applied in bone tissue engineering in aspect of compressive strength. It should be noted that the proper pore structure, bioactive environment, and sufficient mechanical properties need to be balanced adequately to be applied in tissue engineering^[41,95].

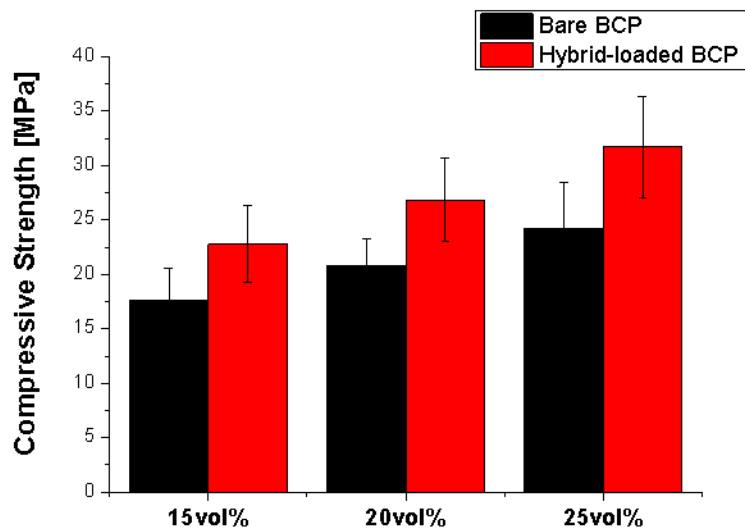


Figure 3.3. Compressive strength of the porous BCP scaffold with various BCP content, before and after hybrid solution coating.

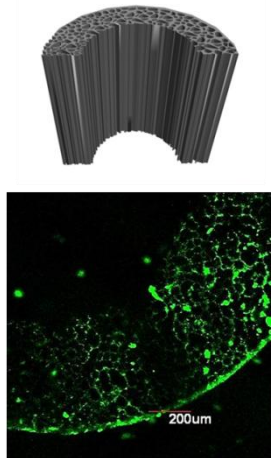
In Vitro Release

The presence of the growth factor in the coating layer was confirmed by CLSM using GFP, as shown in Fig 3.4. The green fluorescence of the growth factor visualized the incorporation of growth factor. It could be observed from CLSM micrograph that the coating layer by hybrid solution containing BMP was uniformly covered and infiltrated the porous BCP scaffold on both outer shell(Fig 3.4.(C)) and inner wall(3.4.(D)).

An appropriate BMP releasing implant material retains BMP at the site for a sufficient time and sufficient level for bone to be induced. It is hypothesized that a burst release followed by a sustained release of factor is most desirable^[96]. The initial burst effect attracts osteoprogenitor cells to defect site and these cells migrate into or near the implanted material to form new tissues. The remaining retained BMP supports the differentiation of cells to the osteoblast phenotype^[97]. It has been reported that long-term release of BMP yields higher bone formation efficiency than short term release at an equivalent dose^[98]. In this view, the BMP release behavior of the prepared samples was investigated in PBS solution up to 90 days with encapsulation of 5 mg/ml of BMP. Fig 3.5 presents the cumulative amount of BMP released from the prepared samples with an equal amount of BMP loading relative to the amount of initial loading. The BMP incorporated in the hybrid coating was rapidly released in the early stage and then slowly after 15 days. In addition, no sign of abrupt release from the surface was observed, which supports successful incorporation of growth factor in PCL/silica hybrid solution. Growth factors, BMP in this study, are known as

water soluble, they can be incorporated in hydrophilic hybrid solution without phase separation. Still, further evaluation is necessary to confirm the effectiveness of the coating solution. Interestingly, there were no significant differences in release behavior up to 5 days regardless of an initial BCP content. However after 7 days, they showed slight different release profile, implying that the release profile is not only affected by the characteristics of the scaffolds but also pore structure. The CLSM observation of BMP-2 released specimen after 14 and 28 days of immersion in PBS and intensity conversion proves the stable BMP-2 loading along the specimen. The increase of initial BCP contents showed decreased pore size in part I. The decreased pore size would be responsible for sustained release of incorporated growth factor.

Before BMP-2(GFP) loading



After BMP-2(GFP) loading

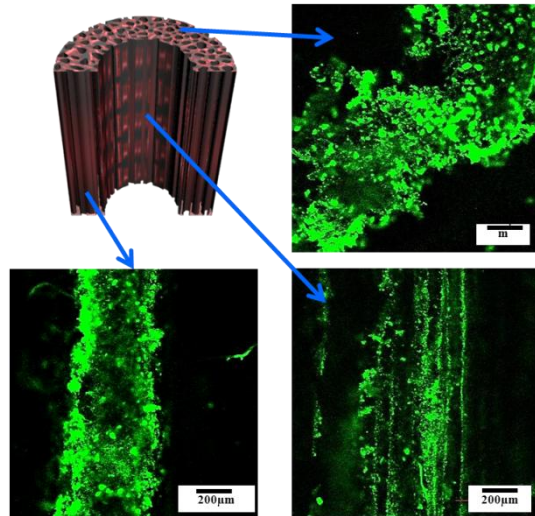


Figure 3.4. Confocal laser scanning microscopy images of GFP adsorbed porous hybrid BCP scaffold.

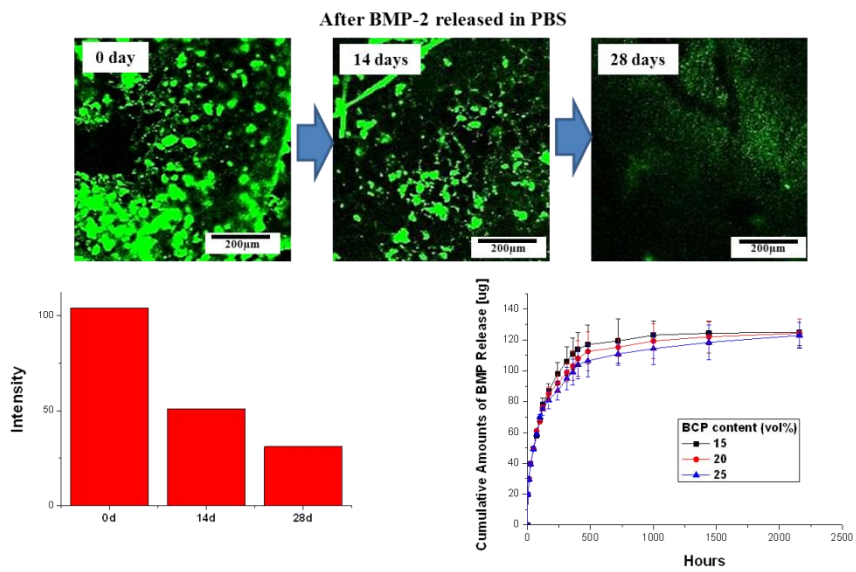


Figure 3.5. Cumulative amounts of BMP released from the PCL/(PCL-silica) hybrid scaffold as a function of time.

In Vitro Cellular Responses

The biocompatibility of the porous hybrid BCP scaffolds was assessed by *in vitro* cell tests in terms of attachment, proliferation, and differentiation of MC3T3-E1 cells. Fig. 3.6 (A)-(C) show typical CLSM images of the MC3T3 cells attached to the porous BCP scaffolds, BCP scaffold coated with PCL/silica solution, and PCL/silica/BMP solution, respectively after 1 day of culturing. All of the produced scaffolds showed that the cells adhered and spread actively on their surfaces, where the red and blue colors represent the actin and the nucleus, respectively. However, the cells appeared to grow and spread more actively on the scaffolds with coating solution.

The degree of cell proliferation on the BCP scaffolds with various conditions is shown in Fig. 3.7 after 5 days of culturing. The level of cell viability increased notably with coating solution. The porous BCP scaffold with BMP showed much higher cell viability than the porous pure BCP scaffold by a factor of ~ 2 . In addition, the ALP activity after 14 days of culturing, which was measured to evaluate the osteoblastic differentiation of the MC3T3-E1 cells, increased remarkably. These findings suggest that the use of biocompatible, bioactive PCL/silica solution could significantly enhance the *in vitro* biocompatibility of the porous BCP scaffolds

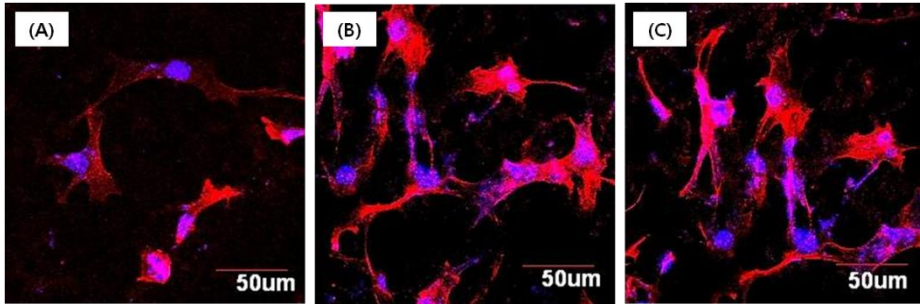


Figure 3.6. CLSM images of the porous hybrid BCP scaffold produced using various conditions, (A) bare BCP scaffold, (B) PCL/silica coated, and (C) PCL/silica/BMP loaded.

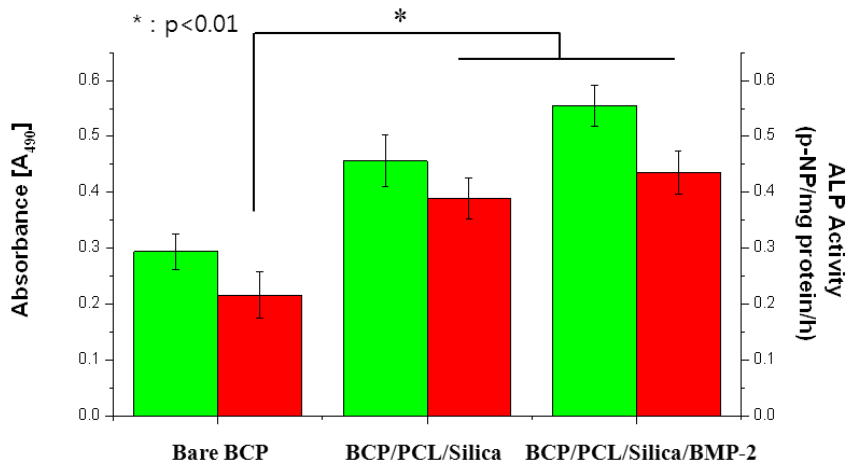


Figure 3.7. Cell viability and ALP activity of the PCL/(PCL-silica) hybrid scaffold with various conditions.

In Vivo Animal Tests

The *in vivo* performance of the BCP/PCL/silica hybrid scaffold was examined using a rat tibial defect model as shown in Fig 3.8. The scaffolds with a diameter of 2.9mm, and length of 5mm were placed in defect site in the tibia. The progression of bone union was determined by radiographic X-ray analysis taken on the post-operative day and 4 weeks after the operation loss of correction, fixation, failure and collapse of osteotomy site on serial plane radiographs(Fig 3.9.). 4 weeks after the operation, bone formation was observed around the defect sites of rat tibia. Radiographic X-ray analysis proved that all scaffolds induced direct bone regeneration without inflammation. The immature new bone and a large quantity of remaining scaffolds were observed. The increase of bone density calculated according the pixel count of BCP control group was $0.05 \pm 0.014 \text{ g/cm}^3$. On the other hand, those of the BCP/PCL/silica and BCP/PCL/silica with BMP-2 group were significantly increased to $0.11 \pm 0.08 \text{ g/cm}^3$ and $0.25 \pm 0.21 \text{ g/cm}^3$, respectively. Although further *in vivo* evaluation and clinical studies will be needed to determine the practical uses of the scaffold, these results imply the potential of biocompatible and bioactive ceramic scaffold coated with organic-inorganic solution to be applied in bone tissue engineering.



Figure 3.8. Photograph of surgical procedure.

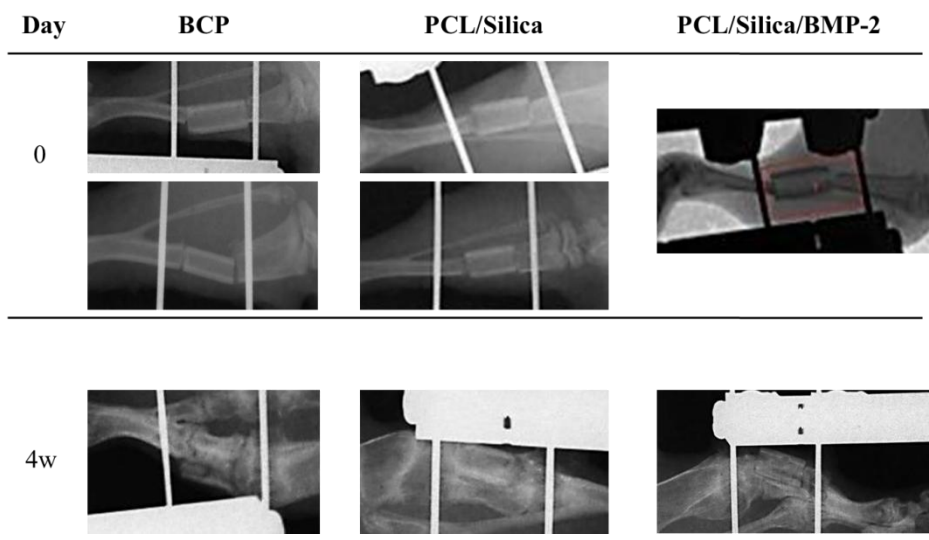


Figure 3.9. Representative 2D radiographs of control, PCL/silica coated, and PCL/silica/BMP-2 coated scaffold in tibia at 0 and 4 weeks of surgery.

4. Conclusions

In order to improve the mechanical strength and biological properties of the porous tubular BCP scaffold prepared from part I, coating with PCL/silica hybrid solution from part II, with growth factor incorporated in the hybrid solution was performed. For uniform coating and successful infiltration, reduced pressure was applied while dip-coating process. The compressive strength and flexural strength were significantly increased after coating process, and cell viability was enhanced. These results highlight that the that coating of hybrid solution on porous BCP scaffold highlights the potential of biocompatible and bioactive ceramic scaffold coated with organic-inorganic solution to be applied in bone tissue engineering.

Conclusion

In this work, we report the preparation and evaluation of the porous BCP/(PCL-silica) hybrid scaffold as potential material for bone tissue engineering. In part I, we fabricated the porous BCP scaffold with aligned pore structure by extruding frozen BCP/camphene body, followed by freeze drying and sintering to densify BCP walls. The camphene dendrite was deformed and elongated during extrusion process, which formed interconnected and unidirectionally aligned pores. In addition, the pore structure and porosities of the samples were tailored by adjusting the initial BCP content in the BCP/camphene slurry and post-treatment at 33 °C. For wider applications, diverse designs of the scaffolds were proposed for customized applications via cylindrical, tubular, and multi-channeled porous BCP ceramics. For their potential use as scaffold, the examinations were performed via pore characteristics, such as porosity, interconnection size, and mechanical tests to evaluate their structural integrity. It should be noted that scaffold with a three-dimensional interconnected pore structure with high porosity, large surface area, and biocompatibility is integral for application in tissue engineering.

In addition, the potential of PCL-silica hybrid solution as the coating material for biomedical application is examined as a membrane type. Biomolecules, such as tetracycline hydrochloride and bone morphogenetic protein-2 (BMP-2) was loaded in the hybrid solution in situ. Poly(ϵ -caprolactone) was chosen as a biopolymer, which is most widely used polymer that can be degraded in human body and with biocompatibility. For inorganic compound in hybrid solution, sol-gel derived silica, which

possesses the mesoporous structure, was used to improve bioactivity of the hybrid material. The PCL/sol-gel derived silica membrane with controlled pore structure were fabricated, characterized, and evaluated in assess of microstructure, wettability, and biological properties. The capability of antibiotic and protein loading was assessed for further applications in this work.

The potential of the BCP/(PCL-silica) hybrid scaffolds as the biomedical implant was examined by coating the porous BCP bioceramic scaffolds with prepared PCL/silica solution. Bone morphogenetic protein-2 (BMP-2) was loaded in the hybrid solution before coating the porous BCP bioceramic. The BCP(PCL-silica) hybrid scaffolds showed significantly improved fracture behavior, which could be used in load bearing part in biomedical field and the enhanced bioactivity of BCP(PCL-silica) hybrid scaffolds was examined by the in vitro cellular test using osteoblast-like cells. Furthermore, in vivo animal study was performed and osseointegration was examined using rat tibial defect model. Fabrication of antibiotic and growth factor eluting material with controlled pore structure is another advantage of this work since in-situ loading of biomolecules to the coating solution is possible. The prepared BCP(PCL-silica) hybrid scaffolds by extrusion and coating process could be a promising material in biomedical applications.

It is still challenging to produce porous scaffold with interconnected pore with proper mechanical strength and biocompatibility. Combining bioceramics with polymeric coating layer would be the one of the solutions, therefore we propose the coating of their surfaces with biopolymer/inorganic

solution. The hybrid solutions were prepared with two major roles: the first is preserving the biocompatible environment for bone cells with addition of inorganic compound to the biopolymer solution, and second, providing the capability of coating solution of the porous scaffold. Based on the results of this study, the camphene-based freeze casting and extrusion method have potential in preparing porous bioceramic scaffold with controlled pore structure. In addition, potentials of bioceramic/(organic-inorganic) hybrid scaffold were suggested. The BCP/(PCL-silica) hybrid scaffold prepared in this study could be a promising material to be used in bone tissue engineering as biomedical implants.

References

- ¹ Hing, K. A. (2005). "Bioceramic bone graft substitutes: Influence of porosity and chemistry." International Journal of Applied Ceramic Technology **2**(3): 184-199.
- ² Sepulveda, P., (1997). "Gelcasting forms for porous ceramics." American Ceramic Society Bulletin **76**(10): 61-65
- ³ Deville, S., E. Saiz, et al. (2006). "Freeze casting of hydroxyapatite scaffolds for bone tissue engineering." Biomaterials **27**(32): 5480-5489.
- ⁴ Wang, C., Y. Xue, et al. (2012). "The enhancement of bone regeneration by a combination of osteoconductivity and osteostimulation using beta-CaSiO₃/beta-Ca₃(PO₄)₂ composite bioceramics." Acta Biomaterialia **8**(1): 350-360.
- ⁵ Puertolas, J. A., J. L. Vadillo, et al. (2011). "Compression behaviour of biphasic calcium phosphate and biphasic calcium phosphate-agarose scaffolds for bone regeneration." Acta Biomaterialia **7**(2): 841-847.
- ⁶ Lin, K., L. Chen, et al. (2011). "Improvement of mechanical properties of macroporous β -tricalcium phosphate bioceramic scaffolds with uniform and interconnected pore structures." Ceramics International **37**(7): 2397-2403.
- ⁷ Studart, A. R., U. T. Gonzenbach, et al. (2006). "Processing Routes to Macroporous Ceramics: A Review." Journal of the American Ceramic Society **89**(6): 1771-1789.
- ⁸ Descamps, M., T. Duhoo, et al. (2008). "Manufacture of macroporous β -

-
- tricalcium phosphate bioceramics." Journal of the European Ceramic Society **28**(1): 149-157.
- ⁹ Liu, X., M. N. Rahaman, et al. (2012). "Porous and strong bioactive glass (13-93) scaffolds prepared by unidirectional freezing of camphene-based suspensions." Acta Biomaterialia **8**(1): 415-423.
- ¹⁰ Jung, H.-D., S.-W. Yook, et al. (2009). "Fabrication of titanium scaffolds with porosity and pore size gradients by sequential freeze casting." Materials Letters **63**(17): 1545-1547.
- ¹¹ Koh, Y.-H., I.-K. Jun, et al. (2006). "In situ Fabrication of a Dense/Porous Bi-layered Ceramic Composite using Freeze Casting of a Ceramic-Camphene Slurry." Journal of the American Ceramic Society **89**(2): 763-766.
- ¹² Li, W.L., Lu, K., Walz, J.Y. (2012). "Freeze casting of porous materials: Review of critical factors in microstructure evolution" International Materials Review **57**(1): 37-60
- ¹³ Deville, S., E. Saiz, et al. (2007). "Ice-templated porous alumina structures." Acta Materialia **55**(6): 1965-1974.
- ¹⁴ Yook, S.-W., H.-E. Kim, et al. (2009). "Fabrication of porous titanium scaffolds with high compressive strength using camphene-based freeze casting." Materials Letters **63**(17): 1502-1504.
- ¹⁵ Soon, Y.-M., K.-H. Shin, et al. (2009). "Compressive strength and processing of camphene-based freeze cast calcium phosphate scaffolds with aligned pores." Materials Letters **63**(17): 1548-1550.
- ¹⁶ Koh, Y.-H., E.-J. Lee, et al. (2006). "Effect of Polystyrene Addition on

-
- Freeze Casting of Ceramic/Camphene Slurry for Ultra-High Porosity Ceramics with Aligned Pore Channels." Journal of the American Ceramic Society **89**(12): 3646-3653.
- ¹⁷ Chen, R., C.-A. Wang, et al. (2007). "Ceramics with Special Porous Structures Fabricated by Freeze-Gelcasting: Using tert-Butyl Alcohol as a Template." Journal of the American Ceramic Society **90**(11): 3478-3484.
- ¹⁸ Hu, L., C.-A. Wang, et al. (2010). "Control of pore channel size during freeze casting of porous YSZ ceramics with unidirectionally aligned channels using different freezing temperatures." Journal of the European Ceramic Society **30**(16): 3389-3396.
- ¹⁹ Deville, S. (2010). "Freeze-Casting of Porous Biomaterials: Structure, Properties and Opportunities." Materials **3**(3): 1913-1927.
- ²⁰ Waschki, T., R. Oberacker, et al. (2009). "Control of Lamellae Spacing During Freeze Casting of Ceramics Using Double-Side Cooling as a Novel Processing Route." Journal of the American Ceramic Society **92**: S79-S84.
- ²¹ Munch, E., E. Saiz, et al. (2009). "Architectural Control of Freeze-Cast Ceramics Through Additives and Templating." Journal of the American Ceramic Society **92**(7): 1534-1539.
- ²² Tang, Y. F., K. Zhao, et al. (2010). "Fabrication of aligned lamellar porous alumina using directional solidification of aqueous slurries with an applied electrostatic field." Journal of the European Ceramic Society **30**(9): 1963-1965.

-
- ²³ Ramay, H. R. and M. Zhang (2004). "Biphasic calcium phosphate nanocomposite porous scaffolds for load-bearing bone tissue engineering." Biomaterials **25**(21): 5171-5180.
- ²⁴ Moon, Y.-W., K.-H. Shin, et al. (2012). "Porous alumina ceramics with highly aligned pores by heat-treating extruded alumina/camphene body at temperature near its solidification point." Journal of the European Ceramic Society **32**(5): 1029-1034.
- ²⁵ Bodde, E. W., J. G. Wolke, et al. (2007). "Bone regeneration of porous beta-tricalcium phosphate (Conduit TCP) and of biphasic calcium phosphate ceramic (Biosel) in trabecular defects in sheep." Journal of biomedical materials research. Part A **82**(3): 711-722.
- ²⁶ Vallet-Regí, M. (2008). "Current trends on porous inorganic materials for biomedical applications." Chemical Engineering Journal **137**(1): 1-3.
- ²⁷ Bose S., Tarafder, S. (2012) "Calcium phosphate ceramic systems in growth factor and drug delivery for bone tissue engineering: A review" Acta Biomaterialia **8**; 1401-1421
- ²⁸ Bellucci, D., V. Cannillo, et al. (2011). "Macroporous Bioglass® -derived scaffolds for bone tissue regeneration." Ceramics International **37**(5): 1575-1585.
- ²⁹ Lee, G. S., J. H. Park, et al. (2011). "Direct deposited porous scaffolds of calcium phosphate cement with alginate for drug delivery and bone tissue engineering." Acta Biomaterialia **7**(8): 3178-3186.
- ³⁰ Bi, L., D. Li, et al. (2011). "Fabrication and characterization of a biphasic

-
- scaffold for osteochondral tissue engineering." Materials Letters **65**(13): 2079-2082.
- ³¹ Emadi, R., F. Tavangarian, et al. (2010). "Nanostructured Forsterite Coating Strengthens Porous Hydroxyapatite for Bone Tissue Engineering." Journal of the American Ceramic Society **93**(9): 2679-2683.
- ³² Zhang, Y., D. Kong, et al. (2012). "Fabrication and properties of porous β -tricalcium phosphate ceramics prepared using a double slip-casting method using slips with different viscosities." Ceramics International **38**(4): 2991-2996.
- ³³ Sung, J.-H., K.-H. Shin, et al. (2011). "Preparation of the reticulated hydroxyapatite ceramics using carbon-coated polymeric sponge with elongated pores as a novel template." Ceramics International **37**(7): 2591-2596.
- ³⁴ Lee, J.-H., H.-E. Kim, et al. (2010). "Improving the strength and biocompatibility of porous titanium scaffolds by creating elongated pores coated with a bioactive, nanoporous TiO₂ layer." Materials Letters **64**(22): 2526-2529.
- ³⁵ Yang, J., J. Yu, et al. (2011). "Recent developments in gelcasting of ceramics." Journal of the European Ceramic Society **31**(14): 2569-2591.
- ³⁶ Guo, X., Z. Zhou, et al. (2012). "Effect of forming process on the integrity of pore-gradient Al₂O₃ ceramic foams by gelcasting." Ceramics International **38**(1): 713-719.

-
- ³⁷ Yoon, B.-H., W.-Y. Choi, et al. (2008). "Aligned porous alumina ceramics with high compressive strengths for bone tissue engineering." Scripta Materialia **58**(7): 537-540.
- ³⁸ Soon, Y.-M., K.-H. Shin, et al. (2011). "Fabrication and compressive strength of porous hydroxyapatite scaffolds with a functionally graded core/shell structure." Journal of the European Ceramic Society **31**(1-2): 13-18.
- ³⁹ Hutmacher, D. W., J. T. Schantz, et al. (2007). "State of the art and future directions of scaffold-based bone engineering from a biomaterials perspective." Journal of tissue engineering and regenerative medicine **1**(4): 245-260.
- ⁴⁰ Han, D, Zhang Q. (2006) "As essential requirement for osteoclasts in refined bone-like tissue reconstruction in vitro", Medical Hypotheses **67**(1); 75-789
- ⁴¹ Dorozhkin, S.V. (2010.) "Bioceramics of calcium orthophosphates" Biomaterials **31**(7) : 1465-1485
- ⁴² Seo, D.S., et al. (2008). "Dissolution of human teeth-derived hydroxyapatite" Ann Biomed Eng **36**(1): 132-140
- ⁴³ Ham, H., I. Chung, et al. (2006). "Macroporous Polymer Thin Film Prepared from Temporarily Stabilized Water-in-Oil Emulsion." Journal of Physics and Chemistry of Solids **110**: 13959-13964.
- ⁴⁴ Colombo, P., A. Arcaro, et al. (2003). "Effect of Hypervelocity Impact on Microcellular Ceramic Foams from a Pre ceramic Polymer." Advanced Engineering Materials **5**(11): 802-805.

-
- ⁴⁵ Ahn, M.-K., K.-H. Shin, et al. (2011). "Highly Porous Biphasic Calcium Phosphate (BCP) Ceramics with Large Interconnected Pores by Freezing Vigorously Foamed BCP Suspensions under Reduced Pressure." Journal of the American Ceramic Society **94**(12): 4154-4156.
- ⁴⁶ Dorsey, S. M., S. Lin-Gibson, et al. (2009). "X-ray microcomputed tomography for the measurement of cell adhesion and proliferation in polymer scaffolds." Biomaterials **30**(16): 2967-2974.
- ⁴⁷ Baas, E., J. H. Kuiper, et al. (2010). "In vitro bone growth responds to local mechanical strain in three-dimensional polymer scaffolds." Journal of Biomechanics **43**(4): 733-739.
- ⁴⁸ Rai, R., A. R. Boccaccini, et al. (2011). "The homopolymer poly(3-hydroxyoctanoate) as a matrix material for soft tissue engineering." Journal of Applied Polymer Science **122**(6): 3606-3617.
- ⁴⁹ Chen, Y., L. Wu, et al. (2010). "An organic/inorganic hybrid mesoporous silica membrane: preparation and characterization." Journal of Porous Materials **18**(2): 251-258.
- ⁵⁰ Helen, W. and J. E. Gough (2008). "Cell viability, proliferation and extracellular matrix production of human annulus fibrosus cells cultured within PDLA/Bioglass (R) composite foam scaffolds in vitro." Acta Biomaterialia **4**(2): 230-243.
- ⁵¹ Laschke, M. W., A. Strohe, et al. (2010). "In vitro and in vivo evaluation of a novel nanosize hydroxyapatite particles/poly(ester-urethane) composite scaffold for bone tissue engineering." Acta Biomaterialia

6(6): 2020-2027.

- ⁵² Wang, Y. B., X. H. Xie, et al. (2011). "Biodegradable CaMgZn bulk metallic glass for potential skeletal application." Acta Biomaterialia **7**(8): 3196-3208.
- ⁵³ Tanaka, S., N. Nakatani, et al. (2011). "Preparation of ordered mesoporous carbon membranes by a soft-templating method." Carbon **49**(10): 3184-3189.
- ⁵⁴ Kawase, T., T. Tanaka, et al. (2011). "Improved adhesion of human cultured periosteal sheets to a porous poly(L-lactic acid) membrane scaffold without the aid of exogenous adhesion biomolecules." Journal of Biomedical Materials Research Part A **98A**(1): 100-113.
- ⁵⁵ Tonda-Turo, C., C. Audisio, et al. (2011). "Porous Poly(epsilon-caprolactone) Nerve Guide Filled with Porous Gelatin Matrix for Nerve Tissue Engineering." Advanced Engineering Materials **13**(5): B151-B164.
- ⁵⁶ Yang, Q., N. Adrus, et al. (2011). "Composites of functional polymeric hydrogels and porous membranes." Journal of Materials Chemistry **21**(9): 2783-2811.
- ⁵⁷ Phong, H. Q., S.-L. Wang, et al. (2010). "Cell behaviors on micro-patterned porous thin films." Materials Science and Engineering: B **169**(1-3): 94-100.
- ⁵⁸ Jack, K. S., S. Velayudhan, et al. (2009). "The fabrication and characterization of biodegradable HA/PHBV nanoparticle-polymer composite scaffolds." Acta Biomaterialia **5**(7): 2657-2667.

-
- ⁵⁹ Lanza R, L. R., Vacanti J (2000). "Principles of tissue engineering." Academic Press
- ⁶⁰ Suárez-González, D., K. Barnhart, et al. (2012). "Controllable mineral coatings on PCL scaffolds as carriers for growth factor release." Biomaterials **33**(2): 713-721.
- ⁶¹ Mattioli-Belmonte, M., G. Vozzi, et al. (2011). "Tuning polycaprolactone–carbon nanotube composites for bone tissue engineering scaffolds." Materials Science and Engineering: C.
- ⁶² Cai, Y. Z., G. R. Zhang, et al. (2012). "Novel biodegradable three-dimensional macroporous scaffold using aligned electrospun nanofibrous yarns for bone tissue engineering." Journal of biomedical materials research. Part A **100**(5): 1187-1194.
- ⁶³ Seyednejad, H., D. Gawlitta, et al. (2012). "In vivo biocompatibility and biodegradation of 3D-printed porous scaffolds based on a hydroxyl-functionalized poly(ϵ -caprolactone)." Biomaterials **33**(17): 4309-4318.
- ⁶⁴ Weng, S., Z. Xia, et al. (2012). "In Situ synthesis of multiblock copolymers of poly(ϵ -caprolactone) with different poly(ether diols) based polyurethane by reactive extrusion." Journal of Applied Polymer Science **124**(5): 3765-3773.
- ⁶⁵ Kang, J., L. Chen, et al. (2012). "Preparation of electrospun polycaprolactone nanofibers with water-soluble eggshell membrane and catechin." Journal of Applied Polymer Science **124**(S1): E83-E90.
- ⁶⁶ Lee, E.-J., S.-H. Teng, et al. (2010). "Nanostructured poly(ϵ -caprolactone)–silica xerogel fibrous membrane for guided bone regeneration." Acta

Biomaterialia **6**(9): 3557-3565.

- ⁶⁷ Kikuchi, M., Y. Koyama, et al. (2004). "Development of guided bone regeneration membrane composed of β -tricalcium phosphate and poly (l-lactide-co-glycolide-co- ϵ -caprolactone) composites." Biomaterials **25**(28): 5979-5986.
- ⁶⁸ Fu, S. Z., X. H. Wang, et al. (2011). "Preparation and properties of nano-hydroxyapatite/PCL-PEG-PCL composite membranes for tissue engineering applications." Journal of Biomedical Materials Research Part B: Applied Biomaterials **97B**(1): 74-83.
- ⁶⁹ Jo, J. H., E. J. Lee, et al. (2009). "In vitro/in vivo biocompatibility and mechanical properties of bioactive glass nanofiber and poly(epsilon-caprolactone) composite materials." Journal of biomedical materials research. Part B, Applied biomaterials **91**(1): 213-220.
- ⁷⁰ Erisken, C., D. M. Kalyon, et al. (2008). "Functionally graded electrospun polycaprolactone and β -tricalcium phosphate nanocomposites for tissue engineering applications." Biomaterials **29**(30): 4065-4073.
- ⁷¹ Yun, H.-s., S.-e. Kim, et al. (2011). "Bioactive glass-poly (ϵ -caprolactone) composite scaffolds with 3 dimensionally hierarchical pore networks." Materials Science and Engineering: C **31**(2): 198-205.
- ⁷² Choi, W.-Y., H.-E. Kim, et al. (2010). "Synthesis of poly(ϵ -caprolactone)/hydroxyapatite nanocomposites using in-situ co-precipitation." Materials Science and Engineering: C **30**(5): 777-780.
- ⁷³ Choi, W.-Y., H.-E. Kim, et al. (2010). "Production and characterization of calcium phosphate (CaP) whisker-reinforced poly(ϵ -caprolactone)

-
- composites as bone regenerative." Materials Science and Engineering: C **30**(8): 1280-1284.
- ⁷⁴ Gerber, T. H. and T. Traykova (2003). "Development and in vivo test of sol-gel derived bone grafting materials." Journal of Sol-Gel Science and Technology **26**: 1173-1178.
- ⁷⁵ Radin, S., G. El-Bassyouni, et al. (2005). "In vivo tissue response to resorbable silica xerogels as controlled-release materials." Biomaterials **26**(9): 1043-1052.
- ⁷⁶ Mishra, A. K. and A. S. Luyt (2008). "Effect of sol-gel derived nano-silica and organic peroxide on the thermal and mechanical properties of low-density polyethylene/wood flour composites." Polymer Degradation and Stability **93**(1): 1-8.
- ⁷⁷ Kotoky, T., B. C. Ray, et al. (2003). "Synthesis and characterization of hybrid organic-inorganic composites derived from polystyrene/copolymers of styrene and methylvinylchlorosilane with silica through the sol-gel method." Journal of Polymer Materials **20**(3): 257-265.
- ⁷⁸ Kortusuo, P., M. Ahola, et al. (2000). "Silica xerogel as an implantable carrier for controlled drug delivery---Evaluation of drug distribution and tissue effects after implantation." Biomaterials **21**: 193-198.
- ⁷⁹ Lee, E.-J., D.-S. Shin, et al. (2009). "Membrane of hybrid chitosan-silica xerogel for guided bone regeneration." Biomaterials **30**(5): 743-750.
- ⁸⁰ Rhee, S., J. Choi, et al. (2002). "Preparation of a bioactive and degradable poly(ϵ -caprolactone)/silica hybrid through a sol gel method."

Biomaterials **23**: 4915-4921.

- ⁸¹ Tang, Z. G., R. A. Black, et al. (2004). "Surface properties and biocompatibility of solvent-cast poly epsilon-caprolactone films." Biomaterials **25**(19): 4741-4748.
- ⁸² Wang, Y., Z. Liu, et al. (2006). "Micropatterned polymer surfaces induced by nonsolvent." Langmuir **22**: 1928-1931.
- ⁸³ Ho, Q. P., S. L. Wang, et al. (2011). "Creation of biofunctionalized micropatterns on poly(methyl methacrylate) by single-step phase separation method." ACS applied materials & interfaces **3**(11): 4496-4503.
- ⁸⁴ Verma, D., K. Katti, et al. (2006). "Bioactivity in in situ hydroxyapatite-polycaprolactone composites." Journal of Biomedical Materials Research Part A **78A**(4): 772-780.
- ⁸⁵ Ivirico, J. L. E., M. S. Sanchez, et al. (2006). "Structure and properties of poly(epsilon-caprolactone) networks with modulated water uptake." Macromolecular Chemistry and Physics **207**(23): 2195-2205.
- ⁸⁶ Shi, X., L. Sun, et al. (2009). "Biodegradable polymeric microcarriers with controllable porous structure for tissue engineering." Macromolecular Bioscience **9**(12): 1211-1218.
- ⁸⁷ Cao, D., Y.-P. Wu, et al. (2011). "Cell adhesive and growth behavior on electrospun nanofibrous scaffolds by designed multifunctional composites." Colloids and Surfaces B: Biointerfaces **84**(1): 26-34.
- ⁸⁸ Isikli, C., Hasirci, N.(2012), "Surface and cell affinity properties of chitosan-gelatin-hydroxyapatite composite films", Key Engineering

Materials 493: 337-342

- ⁸⁹ Venkateswara Rao, A., R. Kalesh, et al. (2003). "Synthesis and Characterization of Hydrophobic TMESTEOS based Silica Aerogels." Journal of Porous Materials **10**: 23-29.
- ⁹⁰ Langer, R., Vacanti, J.P. (2000), "Tissue Engineering" Science **260**: 920-926
- ⁹¹ Chen, Q. Z., I. D. Thompson, et al. (2006). "45S5 Bioglass-derived glass-ceramic scaffolds for bone tissue engineering." Biomaterials **27**(11): 2414-2425.
- ⁹² Ng, A. M., K. K. Tan, et al. (2008). "Differential osteogenic activity of osteoprogenitor cells on HA and TCP/HA scaffold of tissue engineered bone." Journal of biomedical materials research. Part A **85**(2): 301-312.
- ⁹³ Lieberman, J. R., A. Daluiski, et al. (2002). "The role of growth factors in the repair of bone biology and clinical applications." Journal of Bone & Joint Surgery **84A**(6): 1032-1044.
- ⁹⁴ E.B.W. Giesen, Ding, M. Dalstra, T.M.G.J. Van Eijden, Mechanical properties of cancellous bone in the human mandibular condyle are anisotropic, J. Biomech. 34 (2001) 799–803.
- ⁹⁵ Gonzenbach, U. T., A. R. Studart, et al. (2007). "Macroporous Ceramics from Particle-Stabilized Wet Foams." Journal of the American Ceramic Society **90**(1): 16-22.
- ⁹⁶ Li, R. H. and J. M. Wozney (2001). "Delivering on the promise of bone morphogenetic proteins." TRENDS in biotechnology **19**(7): 255-265.

-
- ⁹⁷ Babensee, J. E., L. V. McIntire, et al. (2000). "Growth factor delivery for tissue engineering." Pharmaceutical Research **17**(5): 497-505.
- ⁹⁸ Jeon, O., S. J. Song, et al. (2008). "Long-term delivery enhances in vivo osteogenic efficacy of bone morphogenetic protein-2 compared to short-term delivery." Biochem Biophys Res Commun **369**(2): 774-780.

Curriculum Vitae

Name : Won-Young Choi

Date of Birth : 18 October 1979

Nationality : Republic of Korea

Education

Ph.D. (9/2007 ~ 8/2012)

Strong, Light, Intelligent & Multi Composite Laboratory(SLIM Lab),

School of Materials Science and Engineering, Seoul National Univ.

BioInspired Material(BIM),

Dental Laboratory Science & Engineering, Korea Univ.

Major : Three-Dimensionally Interconnected BCP/(PCL-Silica) Hybrid
Scaffolds with Controlled Microstructure for Biomedical Implant

M.S. (3/2005 ~ 8/2007)

Strong, Light, Intelligent & Multi Composite Laboratory(SLIM Lab),

Major : In-situ Hybridization of Poly(ϵ -caprolactone) and

Nano-Hydroxyapatite(HA) Using Co-precipitation

B.S. (3/1998 ~ 2/2005)

School of Materials Science and Engineering, Seoul National Univ.

Major : Materials Science & Engineering

Research Fields

Organic/Inorganic Hybrid

Porous Ceramics

Ceramic Processing

Biological Evaluation

Other Skills and Experiences

Fabrication

Hand Press, Warm Press, Hot Press, Cold Isostatic Press(CIP),

Atmospheric Furnace, Vertical Furnace, Vacuum Furnace,

Electrospinning, Spin Coating, Extrusion, Shear Mixer, Dip-coating,

Freeze Dryer, Low/High Speed Saw, CNC-machine,

Vacuum Oven, 3D-Printer

Evaluation

X-ray Diffraction (XRD), FT-IR, Thermal Analysis(TGA, DSC, DTA),

Inductively Coupled Plasma Optical Emission Spectrometry(ICP-OES)

Mechanical Test(Tensile/Compressive/Bending Strength), BET,

Optical Microscope, Confocal Laser Scanning Microscopy(CLSM),

Scanning Electron Microscope(SEM),

Transmission Electron Microscope(TEM), Cell Counter, and etc.

Computer Softwares

Word (MS-Word, HNC), Microsoft Excel, Powerpoint, Origin,

Photoshop, 3D-Max

Research Activities

Thesis

Won-Young Choi, Three-Dimensionally Interconnected BCP/(PCL-Silica) Hybrid Scaffolds with Controlled Microstructure for Biomedical Implant, Ph. D. Seoul National University, 2012

International Articles (SCI Journals)

1. Y. H. Koh, J. J. Sun, **W. Y. Choi**, H. E. Kim, *Journal of Power Sources* **161**, 1023-1029 (2006).
2. J. J. Sun, Y. H. Koh, **W. Y. Choi**, H. E. Kim, *Journal of the American Ceramic Society* **89**, 1713-1716 (2006).
3. I. K. Jun, J. H. Song, **W. Y. Choi**, Y. H. Koh, H. E. Kim, H. W. Kim, *Journal of the American Ceramic Society* **90**, 2703-2708 (2007).
4. J. J. Sun, **W. Y. Choi**, H. E. Kim, Y. H. Koh, *Materials Chemistry and Physics* **104**, 288-292 (2007).
5. S. H. Teng, E. J. Lee, C. S. Park, **W. Y. Choi**, D. S. Shin, H. E. Kim, *Journal of Materials Science: Materials in Medicine* **19**, 2453-2461 (2008).
6. B. H. Yoon, **W. Y. Choi**, H. E. Kim, J. H. Kim, Y. H. Koh, *Scripta Materialia* **58**, 537-540 (2008).
7. K. H. Shin, Y. M. Soon, Y. H. Koh, J. H. Lee, **W. Y. Choi**, H. E. Kim, *Materials Letters* **63**, 1341-1343 (2009).
8. **W. Y. Choi**, H. E. Kim, M. J. Kim, U. C. Kim, J. H. Kim, Y. H. Koh, *Materials Science and Engineering C* **30**, 1280-1284 (2010).

-
9. **W. Y. Choi**, H. E. Kim, S. Y. Oh, Y. H. Koh, *Materials Science and Engineering C* **30**, 777-780 (2010).
 10. K. H. Shin, J. H. Sung, Y. H. Koh, J. H. Lee, **W. Y. Choi**, H. E. Kim, *Materials Letters* **64**, 1539-1542 (2010).
 11. H. J. Yoon, U. C. Kim, J. H. Kim, Y. H. Koh, **W. Y. Choi**, H. E. Kim, *Journal of the American Ceramic Society* **93**, 1580-1582 (2010).
 12. M. K. Ahn, K. H. Shin, Y. W. Moon, Y. H. Koh, **W. Y. Choi**, H. E. Kim, *Journal of the American Ceramic Society* **94**, 4154-4156 (2011).
 13. Y. W. Moon, K. H. Shin, Y. H. Koh, **W. Y. Choi**, H. E. Kim, *Journal of the European Ceramic Society* **31**, 1945-1950 (2011).
 14. K. H. Shin, Y. H. Koh, **W. Y. Choi**, H. E. Kim, *Materials Letters* **65**, 1903-1906 (2011).
 15. Y. M. Soon, K. H. Shin, Y. H. Koh, **W. Y. Choi**, H. E. Kim, *Journal of the European Ceramic Society* **31**, 415-419 (2011).
 16. Y. M. Soon, K. H. Shin, Y. H. Koh, J. H. Lee, **W. Y. Choi**, H. E. Kim, *Journal of the European Ceramic Society* **31**, 13-18 (2011).
 17. J. H. Sung, K. H. Shin, Y. H. Koh, **W. Y. Choi**, Y. Jin, H. E. Kim, *Ceramics International* **37**, 2591-2596 (2011).
 18. H. J. Yoon, U. C. Kim, J. H. Kim, Y. H. Koh, **W. Y. Choi**, H. E. Kim, *Nippon Seramikkusu Kyokai Gakujutsu Ronbunshi/Journal of the Ceramic Society of Japan* **119**, 573-576 (2011).
 19. B. Lei, K. H. Shin, D. Y. Noh, I. H. Jo, Y. H. Koh, **W. Y. Choi**, H. E.

-
- Kim, *Journal of Materials Chemistry* **22**, 14133-14140 (2012).
20. B. Lei, K. H. Shin, D. Y. Noh, Y. H. Koh, **W. Y. Choi**, H. E. Kim, *Journal of Biomedical Materials Research - Part B Applied Biomaterials* **100 B**, 967-975 (2012).
21. Y. W. Moon, K. H. Shin, Y. H. Koh, **W. Y. Choi**, H. E. Kim, *Journal of the European Ceramic Society* **32**, 1029-1034 (2012).
22. J. H. Sung, K. H. Shin, Y. W. Moon, Y. H. Koh, **W. Y. Choi**, H. E. Kim, *Ceramics International* **38**, 93-97 (2012).
23. **W. Y. Choi**, H. E. Kim, Y. H. Koh, *Journal of Porous Materials*, Submitted (2012)

Presentations (International & Domestic)

1. **Won-Young Choi**, Hyoun-Ee Kim, Young-Hag Koh. Drug Releasing Intelligent Hybrid Membrane with Controlled Pore Structure. 3rd Asian Biomaterials Congress, September 15-17, Busan, Korea (2011)
2. Young-Wook Moon, Kwan-Ha Shin, **Won-Young Choi**, Hyoun-Ee Kim, Young-Hag Koh. Highly Aligned Porous Alumina Ceramics by Extruding Unidirectionally Frozen Alumina/Camphene Body. 3rd Asian Biomaterials Congress, September 15-17, Busan, Korea (2011)
3. Da-Young Noh, Kwan-Ha Shin, **Won-Young Choi**, Sung-Eun Kim, Hyoun-Ee Kim, Young-Hag Koh. Synthesis Of Sol-Gel Derived Porous, Bioactive Silica Glass/Poly(Ethylene Glycol) Composite Microspheres As

Drug-Eluting Biomaterials. Tissue Engineering and Regenerative Medicine International Society Asia Pacific Meeting 2011 August 3-5, Singapore (2011)

4. Kwan-Ha Shin, Young-Wook Moon, Young-Hag Koh, Sung-Eun Kim, **Won-Young Choi**, Hyoun-Ee Kim. Production Of Porous Poly(ϵ -Caprolactone)/Silica Hybrid Membranes With Patterned Surface Pores. Tissue Engineering and Regenerative Medicine International Society Asia Pacific Meeting 2011 August 3-5, Singapore (2011)

5. Min-Kyung Ahn, Kwan-Ha Shin, Ji-Hyun Sung, Young-Wook Moon, **Won-Young Choi**, Yonghao Kim, Young-Hag Koh. Porous CaP Scaffolds with Tailored Macro-/Micropores. Annual Meeting of Korean Ceramic Society, April 21-22, Suwon, Korea (2011)

6. Ji-Hyun Sung, Kwan-Ha Shin, Young-Wook Moon, Min-Kyung Ahn, **Won-Young Choi**, Young-Hag Koh. Poly(ϵ -caprolactone)-Coated Porous Calcium Phosphate Scaffold for Controlled Drug Release. Annual Meeting of Korean Ceramic Society, April 21-22, Suwon, Korea (2011)

7. **Won-Young Choi**, Jong-Hoon Lee, YongHao Jin, Hyoun-Ee Kim, Young-Hag Koh. Porous Poly(ϵ -caprolactone)/Hydroxyapatite Scaffold with Highly Aligned Pore Structure Using Unidirectional Freeze Drying. Biomaterials - 2011 Annual Meeting and Exposition, April 13-16, Orlando, USA (2011)

8. YongHao Jin, **Won-Young Choi**, Hyoun-Ee Kim, Young-Hag Koh. Porous Calcium Phosphate (CaP) Scaffolds With a Core/Shell Structure Using Indirect Solid Freeform Fabrication(ISFF). Biomaterials 2011 Annual Meeting and Exposition, April 13-16, Orlando, USA (2011)

-
9. **Won-Young Choi**, Hyoun-Ee Kim, Young-Hag Koh. Fabrication and Characterization of Porous Poly(ϵ -caprolactone)/Hydroxyapatite Scaffold with Aligned Pore Structure. Society for Biomaterials 2010 Annual Meeting and Exhibition. April 21-24, Seattle, USA (2010)
 10. **Won-Young Choi**, Hyoun-Ee Kim, Young-Hag Koh. Fabrication of Biological Poly(ϵ -caprolactone)/Hydroxyapatite Porous 3-Dimensional Scaffold. Annual Meeting of Korean Ceramic Society, Korea (2010)
 11. **Won-Young Choi**, Hyoun-Ee Kim, Young-Hag Koh. A Novel Polycaprolactone Film Reinforced with Whisker. Society for Biomaterials 2009 Annual Meeting and Exhibition April 22-25, San Antonio, USA (2009)
 12. **Won-Young Choi**, Hyoun-Ee Kim, Young-Hag Koh. Production and Evaluation of PCL/HA Biological Scaffold. Annual Meeting of Korean Ceramic Society, Korea (2009)
 13. **Won-Young Choi**, Hyoun-Ee Kim, Young-Hag Koh. Preparation of Porous PCL-nano HA Scaffold without Dense Layer by using Freeze-Drying Method. 8th World Biomaterials Congress May 28 – June 1, Amsterdam, Netherlands (2008)
 14. **Won-Young Choi**, Hyoun-Ee Kim, Young-Hag Koh. Preparation of Porous Membrane by using Freeze-Drying Method for Tissue Regeneration. Korean Society of Biomaterials (2007)

국문 초록

기공이 배열된 다공성의 생체세라믹 소재들은 기공의 3차원적인 연결성과 뼈세포의 부착과 성장의 측면에서 유리한 잇점을 가지고 있어서 많은 연구들이 진행되고 있다. 또한 적절한 강도를 갖는 생체세라믹은 조직이 자르는 동안 무너지지 않고 지지해 줄 수 있다. 다양한 종류의 다공성 생체세라믹 제조 공정 중에, 동결 성형은 동결매개체를 활용하여 연결된 기공 채널을 손쉽게 만들 수 있다는 장점을 가지고 있다. 동결 매개체를 고체 상태로 얼린 후, 승화과정을 통해서 제거하여 동결 매개체가 있던 부분이 기공이 되는 형태이다.

본 연구는 기공이 3차원으로 연결된 다공성 인산칼슘 지지체를 캄핀 기반의 동결성형법으로 제조하고 생체의료용 임플란트로써의 활용을 위해 유기/무기 복합체를 코팅하는 방법을 제안하고자 한다. 먼저 고체화된 캄핀/세라믹 슬러리를 상온에서 압출 과정을 통해 기공이 일방향으로 배열된 세라믹 지지체를 제조하였다. 압출 과정은 캄핀 수지상의 일방향 형성을 유도하고 동결건조를 통해 캄핀을 제거하여 기공을 형성시키는 역할을 하였다. 다양한 형태로의 가능성을 확인하기 위해 실린더, 튜브, 다중기공채널 구조의 형태로 제조하고 물성을 평가하였다. 초기 인산칼슘의 양과 후처리 시간에 변화를 주어 기공률, 인산칼슘 벽의 치밀화, 기공 크기 등의 미세 구조를 조절하였다. 제조된 지지체들은

우수한 기계적 강도를 가졌지만 세라믹 자체의 취성과 높은 기공률로 인해 활용의 한계점을 나타내었다. 기계적 물성뿐만 아니라 생체적합성을 가지는 지지체를 제조하기 위해 다공성 인산칼슘 지지체에 하이브리드 용액을 코팅하였다. 인체 내에서 생분해가 가능한 대표적인 생체고분자 중 하나인 폴리카프로락톤과, 메조포로스한 특성을 가지며 생체활성도가 우수한 무기물로 알려져 있는 솔-젤법으로 제조한 실리카를 이용하여 하이브리드 용액을 제조하였다. 효율적인 코팅 용액을 위해 지지막의 형태로 제조하여 미세구조, 친수성, 세포 증식 및 분화능, 약물 및 단백질 담지능 등을 확인하였다.

생체의료용 임플란트 소재로 활용 가능성을 확인하기 위해 다공성 인산칼슘 지지체에 준비된 폴리카프로락톤/실리카 용액을 코팅하여 인산칼슘/(폴리카프로락톤-실리카) 하이브리드 지지체를 제조하였다. 조골형성성장인자인 BMP-2를 *in situ*로 코팅액에 담지하였다. 이는 생체의료용으로 사용하기에 충분한 강도와 파괴 거동을 보였고, 조골세포를 이용한 유사생체실험을 통해 우수한 생체활성도를 갖는 것을 확인하였다. 또한 동물 실험을 통하여 쥐 대퇴부에 결함을 발생시켜 뼈의 증식을 살펴봄으로써 우수한 골재생능을 확인하여 볼 수 있었다.

따라서 본 연구는, 동결성형과 압출과정을 통해 미세구조가 제어된 인산칼슘 지지체의 선제조 후, 생체활성인자를 담지 및 전달할 수 있는 안정적인 폴리카프로락톤-실리카 코팅층을 적용하여 인산칼슘

(폴리카프로락톤-실리카) 하이브리드 지지체를 제조하였고, 이를 통하여 골 조직 재생용 지지체, 생체의료용 임플란트 등 특성화된 임플란트 소재로 적용할 수 있을 것으로 기대된다.

주요어 : 다공성, 동결 성형, 압출법, 생체의료용, 지지체

학번: 2007-30811

감사의 글 (Acknowledgement)

생체 재료라는 단어에 대한 호기심 반 기대 반으로 노크와 함께 시작했던 대학원 생활이 벌써 7년이 되어갑니다. 시원섭섭한 마음과 동시에 아쉬운 마음이 절절히 듭니다. 대학원 생활 동안의 많은 경험들이 앞으로의 제 인생에 중요한 밑거름이 되고 또 도움이 되어줄 것이라 생각합니다. 제 자신이 잘해나갈 수 있을 지에 대한 걱정도 하고 연구에 대한 자신감이 떨어질 때도 있었지만, 주위에서 많은 분들이 도와주시고 믿어주셔서 지금까지 올 수 있었던 것 같습니다. 항상 격려해주시고 조언을 해주셨던 많은 분들께 감사의 말씀을 전하고 싶습니다.

먼저 긴 시간 동안 지도해 주시고 믿어주셨던 김현이 교수님께 감사드립니다. 군 제대하고 복학 후 교수님의 수업을 듣고 교수님의 지도를 받고 싶어서 인사드렸던 기억이 아직도 생생합니다. 연구뿐만이 아니라 연구 외적인 부분에 있어서도 너무 많은 점들을 배웠고, 많이 미흡한 저에게 언제나 기회를 주시고 자신감을 심어주셨기에 항상 감사드립니다. 그 은혜에 보답하기 위해서라도 더욱 열심히 노력하는 제자가 되겠습니다. 사회에 나가서도 항상 교수님의 말씀 가슴 속 깊이 간직하겠습니다.

박사 과정 내내 저에게 큰 힘이 되어 주셨던 고영학 교수님께도 감사드립니다. 교수님의 전폭적인 지지와 믿음이 있었기에 제가 지금까지 올 수 있었습니다. 항상 먼저 배려해주시고 연구에 대

한 자세를 지도해주신 가르침 잊지 않고 더욱 더 최선을 다하겠습니다. 교수님의 가르침을 바탕으로 더더욱 성장하겠습니다.

바쁘신 와중에도 석사와 박사 논문 심사를 모두 맡아주신 홍성현 교수님, 언제나 베풀어주시던 안철희 교수님께도 감사드립니다. 학부 대학원 과정 동안 교수님들의 수업과 지도 덕분에 많은 것을 배울 수 있었습니다. 먼 길도 마다않고 와주셔서 냉철한 지적과 조언을 해주신 김성은 박사님께 감사드립니다. 박사님 덕분에 보다 알차고 완성도 있는 연구를 할 수 있었습니다.

SLIM 실험실에 들어와 훌륭하신 선배분들과 열정적인 후배분들을 만날 수 있었고 배울 수 있어서 큰 행운이었습니다. 아무 것도 모르던 석사 신입생에게 재료에 대해 기초부터 알려주신 김해원 교수님 감사합니다.

졸업하셨지만 마음 따뜻해지는 좋은 기억만 주고 가신 선배님들. 어리버리한 신입생에게 아낌없이 베풀어주시던 종진 형, 늘 먼저 챙겨주시던 근태 형, 정말 친형처럼 응석받아주셨던 치성 형, 창의적과 열정적이 무슨 뜻인지를 보여주신 창번 형, 지금도 용기원 갈 때 마다 신경 써주시는 용호 형, 언제나 한결같던 수희 형, 꾸준한 모습으로 모범이 되어주신 승호 형, 후배라는 이유 하나만으로도 많은 걸 베풀어주시고 나눠주신 창준 형, 저의 이상적인 롤모델이신 병호 형, 자신감있는 모습을 보여주시던 준구 형, 항상 한발짝 먼저 나아가서 도와주시던 재웅 형, 항상 웃는 모습으로 고민 상담해주시던 동근 형, 많은 도움과 조언을 줬던 동윤이, 동갑이지만 누나처럼 챙겨주던 은정이, 언젠가부터 호칭이 애매해진 꼼꼼한 성미, 실험이란 이렇게 하는 것이라라고 매일 보여주신 인국 형, 잔소리 속에 따

뜻한 마음 담아 전해주시던 종재 형, 나이 어린 동생임에도 배울 점이 너무 많던 주하, 모두 감사의 말씀을 전합니다.

가족보다도 더 가족같았던 동기 후배분들께도 감사의 말을 전합니다. 동기지만 늘 앞에서 이끌어주던 신희, 무슨 일을 하던지 특유의 성실함으로 빛을 발하리라 믿어. 대학원 생활 동안 언제나 미안한 마음이 들던 현석이, 어디에 있던지 건강하길 바란다. 자신감과 패기로 뽕뽕 뭉친 지훈이, 회사에 가서도 건승하길~. 인간성 좋고 추진력 뛰어난 연구실의 분위기 메이커 세원이, 얼마 남지 않은 학위 기간 마무리 잘 하리라 믿어. 다재다능하고 실력도 뛰어난 철민이, 덕분에 나름 편하게 마칠 수 있었어 고맙다. 조만간 국방의 의무를 마치고 컴백할 종훈이, 말 안해도 알지? 타지에 와서도 항상 밝은 모습의 원룡이, 긍정적인 마인드는 형도 좀 배워야겠다. 연구실에서 가장 중요한 역할을 하는 현도, 몸 좀 조심하고 지금처럼 열심히 하길 바래. 굶은 일도 마다하지 않고 도와주는 태식이, 무슨 일이든 잘 해 나가리라 믿어. 댄스계를 평정한 지연이, 앞으로 더욱 빛나리라 기대할게. 고대에서 많은 힘이 되어준 영호, 많은 시간을 함께하지는 못했지만 앞장서서 도와주고 챙겨주던 후배님들, 모든 일에 능한 새미, 새 출발을 위해 한걸음 내딛 상복이, 미스코리아스러운 승희, 열정적인 규란이, 어른스럽고 친구같은 봉규, 연구실의 새로운 마스코트 창훈이, 세심하고 마음넓은 성원이, 묵묵히 맡은 일에 최선을 다하는 민호, 친화력 좋고 성격 털털한 설하, 떠오르는 신흥 강호 재욱이, 모두 고맙고 연구와 실험실 생활 잘 해 나가길 바래.

많은 연구 결과들을 도출해주고 가르침을 줬던 수연이, 새로

운 도전을 계속하는 두식 형, 연구실에 굶은 일을 도맡아 해주신 박자혜 씨께도 감사의 말을 전하고 싶습니다.

BIM의 얼굴이었던 어느덧 한 아이의 엄마가 된 영미, 앞으로 계속 BIM의 든직한 기둥이 될 관하, 곧 품절녀가 될 지현이, 물심양면으로 도와주고 죽이 잘 맞던 영옥이, 말은 일이 많아도 다 해결하는 실험실의 새로운 중추가 될 민경이, 힘들었을 텐데도 항상 웃어주던 다영이, 알게 된지 벌써 6년이 된 브레인 인환이, 객지임에도 항상 연구의 모범을 보여준 LeiBo, 재주꾼 커플 대영이, 다숨이, 분야는 다르지만 모범이 되어주시던 완선이 형, 미진 누나. 형 오빠 선배라고 잘 따라주고 도와주던 고려대 후배동생님들에게도 고맙다는 말씀 전하고 싶습니다.

무엇보다도 정말 저에게 힘을 주시고 삶의 원동력인 가족들! 투정부려도 다 받아주시고 안 보이는 곳에서 마음줄이셨을 부모님. 태어나서 지금까지 무한한 사랑을 베풀어주시고 키워주신 아버지, 어머니 감사드리고 사랑합니다. 앞으로도 기대에 어긋나지 않도록 열심히 살겠습니다. 오빠보다도 사회에 먼저 발을 내딛고 의젓해진 내 하나뿐인 동생. 그 누구보다 의지가 되고 힘이 되어줘서 고마워. 할아버지, 항상 건강하시고 자주 연락드릴게요.

학생 신분임에도 불구하고 나를 믿고 지금까지 따라와준 사랑스런 내반쪽. 자기가 있어서 내가 계속 앞으로 나아갈 수 있었어요. 이제는 내가 앞장서서 달릴게요. 사랑해요. 금쪽 같은 선유랑 자윤이. 아빠는 두 딸들이 너무나 자랑스럽습니다. 지금처럼 건강하고 사랑스럽게 자라주세요. 어머니님, 아버지님, 큰형님, 작은형님, 바쁘다는 핑계로 연락도 자주 못드리고 찾아뵙지 못해서 죄송합니

다. 보여주셨던 따뜻한 마음과 은혜 보답하겠습니다. 항상 행복하고 건강하세요.

이 외에도 미처 글로 답지 못한 여러 지인분들께 감사의 뜻을 전하고 싶습니다.